76. Semileptonic b-Hadron Decays, Determination of V_{cb}, V_{ub}

Revised August 2023 by A.X. El-Khadra (Physics, Illinois U.) and P. Urquijo (School of Phys. U. of Melbourne).

76.1 Introduction

Precision determinations of $|V_{ub}|$ and $|V_{cb}|$ are central to testing the CKM sector of the Standard Model, and complement the measurements of CP asymmetries in B decays. The length of the side of the unitarity triangle opposite the well-measured angle β is proportional to the ratio $|V_{ub}|/|V_{cb}|$; its precise determination is a high priority of the heavy-flavor physics program.

The transitions $b \to c\ell\bar{\nu}_\ell$ and $b \to u\ell\bar{\nu}_\ell$ ($\ell = e, \mu$) each provide two avenues for determining these CKM matrix elements, namely through measurements of inclusive decay rates, $\bar{B} \to X\ell\bar{\nu}_\ell$ with a sum over all possible hadronic states X or of exclusive rates, where the final state hadron is a specific meson ($X = D$, D^*, π, ρ etc.).

Purely leptonic decays, such as $B_c^- \to \tau\bar{\nu}$, $B^- \to \tau\bar{\nu}$, and $B^- \to \mu\bar{\nu}$, provide a third avenue that is theoretically very simple (see the RPP mini-review [1]). However, we do not use this information at present since none of the measurements have reached a competitive level of precision. Hence the results presented here are solely obtained from exclusive and inclusive semileptonic b-hadron decays. This article and the values quoted here update the previous review [2].

The theoretical methods underlying the different determinations of $|V_{qb}|$ are quite mature. The theoretical approach for inclusive determinations uses the fact that the mass m_b of the b quark is large compared to the scale $\Lambda_{\rm QCD}$ that determines low-energy hadronic physics. Thus the basis for precise calculations is a systematic expansion in powers of Λ/m_b, where $\Lambda \sim 500 - 700$ MeV is a hadronic scale of the order of $\Lambda_{\rm QCD}$. Such an expansion can be formulated in the framework of an effective field theory which is described in a separate RPP mini-review [3]. Exclusive determinations rely on non-perturbatively calculated form factors, that encode the low-energy dynamics of the hadronic transition. Here, lattice QCD provides an, in principle, ab-initio method to calculate the non-perturbative QCD contributions to the exclusive decay amplitudes. Thanks to a combination of improved theoretical methods, better algorithms, and large increases in computational power, precise lattice QCD results are now available for the processes that are used in exclusive $|V_{ub}|$ and $|V_{cb}|$ determinations. State-of-the-art lattice QCD calculations are based on gauge-field ensembles that include realistic sea quark effects for degenerate up/down and strange quarks (aka $2+1$-flavor ensembles), and increasingly, also for charm (aka $2+1+1$-flavor ensembles). They employ ensembles generated at three (or more) lattice spacings, different spatial volumes, among other parameter variations to allow for quantification of the underlying systematic errors, and include detailed systematic error analyses. This is described in a separate RPP mini-review [4]. The lattice-QCD results discussed in this review are all state-of-the art with fully quantified uncertainties, and therefore play a central role in exclusive $|V_{qb}|$ determinations. In the case of exclusive $\bar{B} \to D^{(*)}\ell\bar{\nu}_\ell$ decays, heavy quark symmetry (HQS) and heavy quark effective theory (HQET) yield constraints on the form factors that can be used to improve exclusive $|V_{cb}|$ determinations, especially when lattice QCD form factor results are incomplete, as was the case until very recently for $\bar{B} \to D^*\ell\bar{\nu}_\ell$. Light-cone sum rules (LCSR) provide another nonperturbative approach to compute form factors. However, while the lattice-QCD results employed in this review have well-quantified uncertainties, LCSR results suffer, in general, from hard-to-quantify systematic errors. The two methods typically provide results in opposite regions of phase space. Lattice-QCD calculations work best at low hadronic recoil or high momentum transfer (q^2) to the leptons, while LCSR calculations provide estimates at high recoil, near $q^2 = 0$. In general, we don't use form factor inputs obtained from

LCSR in this review.

The measurements discussed in this review are of branching fractions, ratios of branching fractions, and decay kinematic distributions. The determinations of $|V_{cb}|$ and $|V_{ub}|$ also require a measurement of the total decay widths of the corresponding b hadrons, determined from lifetimes, which is the subject of a separate RPP mini-review [5]. The measurements of inclusive semileptonic decays relevant to this review come primarily from e^+e^- B factories operating at the $\Upsilon(4S)$ resonance, while the measurements of exclusive semileptonic decays come from both the e^+e^- B factories and from the LHCb experiment at CERN.

Semileptonic B-meson decay amplitudes to electrons and muons are well measured and consistent with Standard Model W-boson exchange. As they are expected to be insensitive to the effects of non-Standard-Model physics, they are used to extract $|V_{qb}|$. However, semileptonic decays to tau-lepton final states, such as $\bar{B} \to D^{(*)}\tau\bar{\nu}_\tau$, may be sensitive to effects from beyond the Standard Model particles due to the large mass of the τ lepton. The currently observed tensions between Standard Model theory and experiment for these decays indicate that semitauonic decays must be studied further. For rare decays, tests of lepton-flavor universality violations (LFUV) in ratios involving μ/e final states provide CKM-free tests of the SM. These and other flavor dependent angular analyses are also included in this review.

Many of the numerical results quoted in this review have been provided by the Heavy Flavor Averaging Group (HFLAV) [6].

76.2 Determination of $|V_{cb}|$

Summary: The determination of $|V_{cb}|$ from inclusive decays has a relative uncertainty of about 1.5%; the limitations arise mainly from our ignorance of higher-order perturbative and non-perturbative corrections. Exclusive $\bar{B} \to D^*\ell\bar{\nu}_\ell$ decays provide a determination of $|V_{cb}|$ with a relative precision of about 2%, with comparable contributions from theory and experiment to the total uncertainty; the value determined from $\bar{B} \to D\ell\bar{\nu}_\ell$ decays is consistent and has an uncertainty of 2.5%. The values obtained from the inclusive and exclusive B decay determinations discussed below are:

$$|V_{cb}| = (42.2 \pm 0.5) \times 10^{-3} \quad \text{(inclusive)} \tag{76.1}$$

$$|V_{cb}| = (39.8 \pm 0.6) \times 10^{-3} \quad \text{(exclusive)}. \tag{76.2}$$

An average of these determinations has $p(\chi^2) = 1\%$, so we scale the error by $\sqrt{\chi^2/1} = 3.0$ to find

$$|V_{cb}| = (41.1 \pm 1.2) \times 10^{-3} \quad \text{(average)}. \tag{76.3}$$

Given the only marginal consistency, of approximately 3.0 σ, this average should be treated with caution.

76.2.1 $|V_{cb}|$ *from exclusive decays*

Exclusive determinations of $|V_{cb}|$ make use of semileptonic B decays into the ground state charmed mesons D and D^*. The corresponding hadronic matrix elements can be parameterized in terms of six independent form factors, which depend on the variable $w \equiv v \cdot v'$, where v and v' are the four velocities of the initial and final-state hadrons. In the rest frame of the decay this variable corresponds to the Lorentz factor of the final state $D^{(*)}$ meson. Determinations of $|V_{cb}|$ from experimental measurements of $\bar{B} \to D^{(*)}\ell\bar{\nu}_\ell$ decay rates require precise knowledge of these form factors. Fortunately, lattice QCD results for all relevant form factors, including their recoil dependence, are now available [7–12]. Heavy Quark Symmetry (HQS) [13,14] predicts that in the infinite mass limit the six form factors collapse into a single one, which is normalized at the "zero recoil point" $w = 1$, the point of maximum momentum transfer to the leptons. Heavy

Quark Effective Theory (HQET) provides a framework for obtaining the corrections to the HQS prediction in a systematic expansion in powers of $\Lambda_{\rm QCD}/m_c$ which is discussed in a separate RPP mini-review [3].

76.2.2 $\bar{B} \to D^* \ell \bar{\nu}_\ell$

The decay rate for $\bar{B} \to D^* \ell \bar{\nu}_\ell$, assuming massless leptons, is given by

$$\frac{d\Gamma}{dw}(\bar{B} \to D^* \ell \bar{\nu}_\ell) = \frac{G_F^2 m_B^5}{48\pi^3} |V_{cb}|^2 |\eta_{\rm EW}|^2 (w^2-1)^{1/2} P(w) |\mathcal{F}(w)|^2, \tag{76.4}$$

where $P(w)$ is a phase space factor,

$$P(w) = r^3 (1-r)^2 (w+1)^2 \left(1 + \frac{4w}{w+1}\frac{1-2rw+r^2}{(1-r)^2}\right), \tag{76.5}$$

with $r = m_{D^*}/m_B$. The decay amplitude $\mathcal{F}(w)$ can be expressed in terms of the form factors which parametrize the vector and axial vector current matrix elements

$$\frac{\langle D^*(v',\epsilon)|\bar{c}\gamma^\mu b|B(v)\rangle}{\sqrt{m_B m_{D^*}}} = h_V(w)\, \varepsilon^{\mu\nu\rho\sigma} v_{B,\nu} v_{D^*,\rho} \epsilon^*_\sigma\,, \tag{76.6}$$

$$\frac{\langle D^*(v',\epsilon)|\bar{c}\gamma^\mu\gamma^5 b|B(v)\rangle}{\sqrt{m_B m_{D^*}}} = i h_{A_1}(w)\,(1+w)\epsilon^{*\mu} - i\,[h_{A_2}(w) v_B^\mu + h_{A_3}(w) v_{D^*}^\mu]\,\epsilon^*\cdot v_B\,, \tag{76.7}$$

and the ratios

$$R_1(w) = \frac{h_V(w)}{h_{A_1}(w)}\,, \quad R_2(w) = \frac{h_{A_3}(w) + r\, h_{A_2}(w)}{h_{A_1}(w)}\,, \tag{76.8}$$

as

$$\begin{aligned} P(w)|\mathcal{F}(w)|^2 \;=\;& |h_{A_1}(w)|^2 \\ & \times \left\{ 2\frac{r^2-2rw+1}{(1-r)^2}\left[1 + \frac{w-1}{w+1} R_1^2(w)\right] + \left[1 + \frac{w-1}{1-r}(1-R_2(w))\right]^2 \right\}. \end{aligned} \tag{76.9}$$

Note that $\mathcal{F}$ at $w = 1$ is unity by HQS in the infinite-mass limit [15–18]. The effect of assuming massless leptons is typically very small, but for the muon case can be non-negligible in fits to data at high hadronic recoil.

The factor $\eta_{\rm EW} = 1.0066 \pm 0.0050$ accounts for the leading electroweak corrections to the four-fermion operator mediating the semileptonic decay [19], and includes an estimated uncertainty for missing long-distance and structure-dependent QED corrections [20]. While some QED radiative corrections are included in the experimental analysis, the Coulomb correction, which arises when the final-state hadron is charged, is not taken into account.

The determination of $|V_{cb}|$ requires knowledge of the normalization, where one commonly uses a theoretical calculation of the zero recoil input, $\mathcal{F}(1)$. Theoretical knowledge of the shapes of the form factors provides crucial compatibility checks between theory and experiment, and improves the precision of the determinations.

Model-independent shape parametrizations of the form factors make use of analyticity and unitarity constraints and are expressed in terms of the variable

$$z = \frac{\sqrt{w+1} - \sqrt{2N}}{\sqrt{w+1} + \sqrt{2N}}\,, \tag{76.10}$$

originating from a conformal transformation, where $N = (t_+ - t_0)/(t_+ - t_-)$, $t_\pm = (m_B \pm m_{D^*})^2$, and the choice of t_0 determines the kinematic point at which $z = 0$. The form factors (generically denoted as F) may then be written as [21–25]

$$F(z) = \frac{1}{P_F(z)\phi_F(z)} \sum_{n=0}^{\infty} a_n z^n \tag{76.11}$$

where the sum is bounded, $\sum |a_n|^2 < 1$. Furthermore, the function $P_F(z)$ takes into account the resonances in the $(\bar{c}b)$ system below the $\bar{D}B$ threshold, and the weighting functions $\phi_F(z)$ are derived from the unitarity constraint on the corresponding form factor. With the conventional choice $N = 1$, $z = 0$ when $w = 1$ and kinematic range of the decay corresponds to $0 \leq z \leq 0.06$. As a result, only very few terms are needed in the series in z. We refer to Eq. (76.11) as the "BGL" expansion.

The Caprini-Lellouch-Neubert (CLN) parametrization [26] yields a simple form

$$h_{A_1}(w) = h_{A_1}(1)\left[1 - 8\rho^2 z + (53\rho^2 - 15)z^2 - (231\rho^2 - 91)z^3\right] \tag{76.12}$$

with the slope ρ and normalization $h_{A_1}(1)$ as the only parameters, albeit at the cost of introducing model dependence. Furthermore, the ratios $R_1(w)$ and $R_2(w)$ are expanded in $w-1$. However, this simple CLN parametrization does not account for higher-order corrections in the $1/m_{c/b}$ expansion, which are now relevant [25,27–33]. In addition, the numerical values of the coefficients use outdated knowledge and should include uncertainties. Thus, this report focuses on recent analyses that employ different combinations of HQET expansions through $\mathcal{O}(\alpha_s/m_{b,c}, 1/m_{b,c}^2)$, lattice form factors at non-zero recoil, as well as the model-independent BGL expansion. Typical fits include up to three parameters a_n in Eq. (76.11) for the different form factors.

There now exist three independent lattice QCD calculations by Fermilab/MILC [9], HPQCD [10], and JLQCD [11] of the $\bar{B} \to D^* \ell \bar{\nu}_\ell$ form factors at non-zero recoil. The three groups each employ statistically independent gauge-field ensembles and use different lattice actions for the heavy and light quarks. To obtain results in the continuum and at the physical point, all three analyses first perform chiral-continuum fits and systematic error studies on the corresponding lattice form factor data. The resulting continuum form factors are smooth functions (bands) obtained over recoil ranges which depend on the respective simulation details. In a second step, BGL-expansion fits are used to obtain the form factors over the entire recoil range. We note that the interplay between choices for the ChPT-based continuum extrapolations and BGL coefficients needs further investigation [34]. A comparison of the resulting $|\mathcal{F}(w)|^2$ amplitudes is shown in Fig. 76.1. While the lattice results are reasonably consistent in the low-recoil region, there is some variation in the slopes, as is evident from the spread between the bands at large recoil.

Prior lattice calculations obtained results for only the form factor at the zero-recoil point, $\mathcal{F}(1)$, [20,35] with a total uncertainty at the (1-2)% level. A weighted average of the $\mathcal{F}(1)$ results from Refs. [10,11,20] yields

$$\mathcal{F}(1) = 0.903 \pm 0.012\,. \tag{76.13}$$

The lattice QCD results in Refs. [9–11] appeared (or were published) after the most recent FLAG review [36], and will therefore be included in the next FLAG review. Non-lattice estimates based on zero-recoil sum rules for the form factor tend to yield lower central values for $\mathcal{F}(1)$ [37–39]. The sum rules indicate that $\mathcal{F}(1) < 0.92$ [37,38,40,41], while an explicit estimate that includes excited state contributions yields $\mathcal{F}(1) \approx 0.86$ [39,42]. Lattice-QCD form factors at non-zero recoil provide valuable shape constraints, and hence enable more refined $|V_{cb}|$ determinations. However, since they were not available until recently, some $|V_{cb}|$ determinations in the literature use the value for

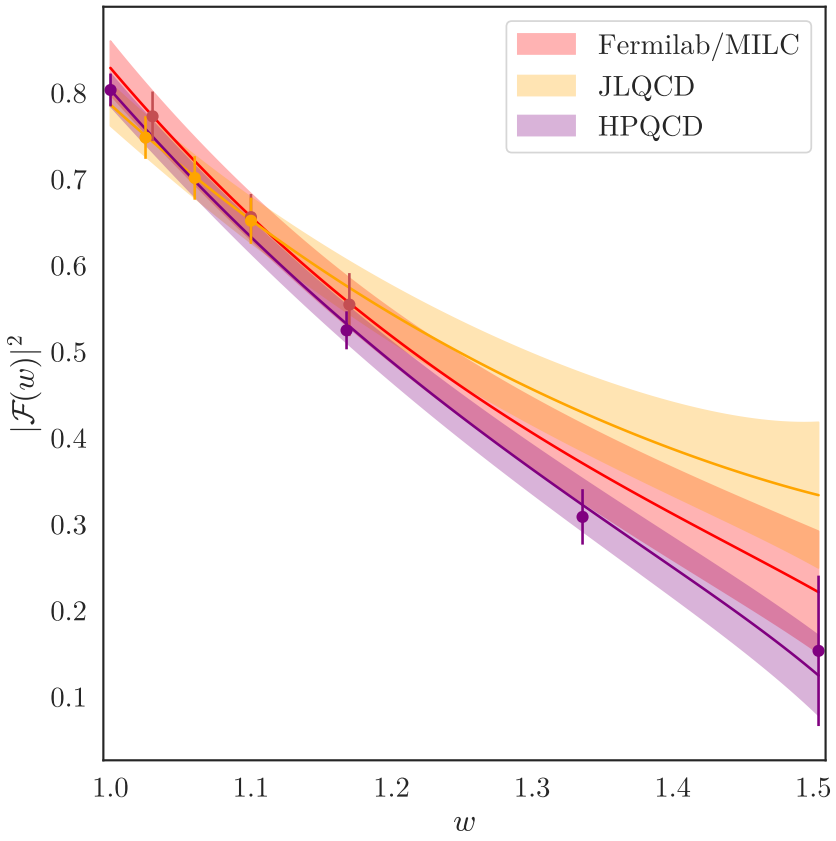

Figure 76.1: Comparison of lattice QCD results for $|\mathcal{F}(w)|^2$ obtained by the Fermilab Lattice and MILC collaborations (red), HPQCD (purple), and JLQCD (yellow). Plot courtesy of A. Vaquero.

$\mathcal{F}(1)$ from Eq. (76.13) as the only quantitative lattice input. We discuss these first, before turning to results for $|V_{cb}|$ which employ the lattice-QCD form factors at non-zero recoil from Refs. [9–11].

While Light Cone Sum Rules (LCSR) can provide constraints on the form factors at maximum recoil, the underlying systematic errors are not fully quantified. A modern LCSR calculation [43] quotes uncertainties in the $\lesssim 20\%$ range for the $\bar{B} \to D^{(*)}\ell\bar{\nu}_\ell$ form factors at $q^2 = 0$.

Dispersive methods [44] can also be used to provide additional constraints on form factors calculated in lattice QCD. Recent work [45, 46] introduces the dispersive matrix method, which includes a strategy for computing the susceptibilities that are also needed inputs in z-expansion fits. They are calculable in lattice QCD from two-point correlation functions, which must be analyzed with the same care as the form factors themselves. The susceptibilities have also been computed in perturbative QCD in Ref. [47]. The two sets of results in Refs. [46, 47] differ in some cases outside of the quoted error bars, with a significance of up to 2.5σ. A test of the dispersive matrix approach for the $D \to K\ell\nu$ form factors, which can be computed in lattice-QCD over the entire kinematic range, is presented in Ref. [45]. The implementation of the dispersive matrix in Ref. [48] imposes unitarity constraints on the input data via a so-called unitarity filter. The filter has the effect of altering the shapes of the form factor bands while reducing the uncertainties from extrapolating the form factors over the entire kinematic range. Subsequently, the authors of Ref. [48] determine $|V_{cb}|$ from a bin-by-bin analysis of the experimental data, which avoids the common shape constraints in joint z-expansion fits. In follow-up work, this method has also been applied to other

semileptonic decay channels [49–51]. A more recent proposal [52] employs Bayesian inference to implement unitarity constraints, which allows for a straightforward combination of inputs from multiple lattice calculations while including experimental data in joint z-expansion fits.

Many experiments [53–65] have measured the differential decay rate as a function of w, employing a variety of methods: using either B^+ or B^0 decays, with or without B-tagging, and with or without explicit reconstruction of the transition pion from $D^* \to D$ decays. In Ref. [6] a subset of the available experimental measurements were input to a four-dimensional fit for $\eta_{\rm EW}\mathcal{F}(1)|V_{cb}|$, $\rho^2_{A_1}$ and the form-factor ratios $R_1 \propto A_2/A_1$ and $R_2 \propto V/A_1$. The fit has a p-value of 0.9%, so we scale the uncertainty by a factor $\sqrt{\chi^2/23}$ to give $\eta_{\rm EW}\mathcal{F}(1)\,|V_{cb}| = (35.00 \pm 0.49) \times 10^{-3}$ (CLN).

The leading sources of uncertainty on $\eta_{\rm EW}\mathcal{F}(1)\,|V_{cb}|$ are due to detection efficiencies and $D^{(*)}$ decay branching fractions. Note that the $\bar{B} \to D^*\ell\bar{\nu}_\ell$ form factor in the fit is parameterized using the CLN form, which has the drawbacks discussed previously.

Using the value from Eq. (76.13) for $\mathcal{F}(1)$ and accounting for the electroweak correction gives

$$|V_{cb}| = (38.5 \pm 0.5 \pm 0.6) \times 10^{-3} \ (\bar{B} \to D^*\ell\bar{\nu}_\ell,\ \text{LQCD, CLN}). \tag{76.14}$$

A safer approach is to use the more general BGL form-factor parameterization [22–25, 29]. The BABAR and Belle experiments have published analyses with BGL based parametrizations at a given order in the expansion [62–64]. A preliminary measurement from Belle II [65] has also been performed with a BGL based parametrization. The main results from these measurements are summarised in Table 76.1 after multiplying through the value of $\mathcal{F}(1)$ quoted in the nominal result of each respective study. These results have not yet been combined by the Heavy Flavor Averaging Group.

The Belle analysis [62] and the Belle II analysis [65] are both based on untagged approaches in the mode $\bar{B}^0 \to D^{*+}\ell\bar{\nu}_\ell$ and measure 1-d projections in bins of the hadronic recoil w, and angular variables $\cos\theta_\ell$, $\cos\theta_V$, and χ. The BABAR analysis [63] and the recent Belle analysis [64] are based on hadronic tagged samples using both charged and neutral B decays. BABAR performs a full 4-d unbinned analysis of neutral and charged B decay modes, while Belle uses unfolded 1-d projections of w, $\cos\theta_\ell$, $\cos\theta_V$, and χ. Only the BGL form factors are directly determined in these tagged analysis, not the normalization, which is taken from the world average $\bar{B} \to D^*\ell\bar{\nu}_\ell$ branching fractions.

Table 76.1: $\mathcal{F}(1)\eta_{EW}|V_{cb}|$ results from $B \to D^*\ell\nu$ with BGL expansion fits. Note that the tagged analyses combined results from B^- and $\bar{B}^0$ decays, while the untagged analyses study only $\bar{B}^0$ decays. The final column listed the non-zero recoil lattice QCD data used in each study.

Measurement	Tag	$\mathcal{F}(1)\eta_{EW}\lvert V_{cb}\rvert \times 10^3$	Fit inputs
Belle [66]	Untagged	35.22 ± 0.95	FNAL/MILC [20]
Babar [63]	Tagged	34.98 ± 0.65	
Belle [64]	Tagged	37.00 ± 0.56	FNAL/MILC [9], HPQCD [10], JLQCD [11]
Belle II [65]	Untagged	36.94 ± 0.91	FNAL/MILC [9]

The studies in Refs. [62, 64, 65] publish the fully-differential decay rate data and associated covariance matrices. The BGL fit results in the Belle, Belle II and BABAR measurements are all consistent with corresponding results from fits with the CLN parametrization, Eq. (76.14). Each study reports fit results at low order in the three BGL expansion terms when non-zero lattice data is not used as an additional constraint, ranging from zero-order to second-order. Studies of the impact of higher order expansions based on the Belle published decay rate data have been reported

in Refs. [30,31], as well as in the recent Belle and Belle II studies [64,65], where it is shown that the fit uncertainty on $|V_{cb}|$ increases substantially with respect to the results reported at lower order, while the parameter correlations approach 1. This is due to larger number of degrees of freedom allowed in the higher order expansions, which are not sufficiently constrained without lattice-QCD inputs at nonzero recoil.

In Ref. [9], BGL expansion fits to the FNAL/MILC lattice QCD form factors show that they are insensitive to truncation effects beyond quadratic order. These form factors were subsequently used in Ref. [9] to extract $|V_{cb}|$ from combined BGL fits to the Belle [62] and synthetic BABAR [63] $\bar{B} \to D^* \ell \bar{\nu}_\ell$ data, yielding $|V_{cb}| = (38.74 \pm 0.78) \times 10^{-3}$. The p-values for the combined (experiment+lattice QCD) BGL fits reported in Ref. [9] are small, reflecting tensions between the data sets. For a fit combining only the Belle data with the lattice-QCD form factors, Ref. [9] quotes $|V_{cb}| = 38.60(86) \times 10^{-3}$, while a fit combining the experimental data with only the lattice QCD $\mathcal{F}(1)$ yields $|V_{cb}| = 39.75(92) \times 10^{-3}$. Similarly, Refs. [10, 11] present analyses based on the BGL expansion, combining the respective lattice form factor results with the new Belle data [64]. The HPQCD collaboration [10] reports $|V_{cb}| = 39.31(74) \times 10^{-3}$, while the JLQCD collaboration [11] reports $|V_{cb}| = 39.19(90) \times 10^{-3}$. All these determinations are consistent with the result presented in Eq. (76.15) as well as with other exclusive determinations, where the HPQCD value needs to be shifted due to their inclusion of the Coulomb factor in η_{EW}. As noted in Refs. [9–11,64,65], the form factor shapes and $R_2(w)$ ratio predicted from FNAL/MILC [9] and HPQCD [10] are in tension with experimental data yielding small p-values, while those from JLQCD [11] are not. Furthermore, the $R_2(w)$ ratio results from Refs. [9,10] are also in tension with HQET expectations (see, for example, Refs. [30, 32, 33, 67]). These tensions must be understood better in order to improve the precision of $|V_{cb}|$ extractions. Indeed, ongoing experimental analyses as well as theoretical work may resolve them in the near future.

For this review, we take a naive combination of the results in Table 76.1, assuming minimal correlations between measurements, and correct for the value of $\mathcal{F}(1)\eta_{EW}$. In the future we expect HFLAV to perform a combined global fit analysis. The combination has a p-value of 8%. The nominal result for $|V_{cb}|$ is therefore

$$|V_{cb}| = (39.7 \pm 0.7) \times 10^{-3} \ (\bar{B} \to D^* \ell \bar{\nu}_\ell, \ \text{LQCD}, \text{BGL}), \tag{76.15}$$

where the uncertainty contains contributions from experimental, lattice QCD, and $\eta_{\rm EW}$ sources. We note that despite the improvements in the experimental data, theoretical inputs, and $|V_{cb}|$ extraction methods, this new exclusive determination of $|V_{cb}|$, while higher in central value compared to earlier ones, is still in tension with the inclusive determinations discussed in Section 76.2.5 and summarized in Eq. (76.32).

76.2.3 $\bar{B} \to D \ell \bar{\nu}_\ell$

The differential rate for $\bar{B} \to D \ell \bar{\nu}_\ell$ is given by

$$\frac{d\Gamma}{dw}(\bar{B} \to D \ell \bar{\nu}_\ell) = \frac{G_F^2}{48\pi^3} |V_{cb}|^2 (m_B + m_D)^2 m_D^3 (w^2 - 1)^{3/2} (\eta_{\rm EW} \mathcal{G}(w))^2. \tag{76.16}$$

The form factor is defined in terms of

$$\frac{\langle D(v') | \bar{c} \gamma^\mu b | B(v) \rangle}{\sqrt{m_B m_D}} = h_+(w) \, (v_B + v_D)^\mu + \, h_-(w) \, (v_B - v_D)^\mu \tag{76.17}$$

and reads

$$\mathcal{G}(w) = h_+(w) - \frac{m_B - m_D}{m_B + m_D} h_-(w), \tag{76.18}$$

where $h_+(1)$ is normalized to unity due to HQS and $h_-(1)$ vanishes in the infinite-mass limit. Thus

$$\mathcal{G}(1) = 1 + \mathcal{O}\left(\left(\frac{m_B - m_D}{m_B + m_D}\right)^2 \frac{\Lambda_{\rm QCD}}{m_c}\right) \tag{76.19}$$

and the corrections to the HQS prediction are of order $\Lambda_{\rm QCD}/m_c$ in contrast to the case of $\mathcal{F}(1)$. The lattice-QCD result for the normalization, $\mathcal{G}(1)$, obtained in Ref. [7] is

$$\mathcal{G}(1) = 1.054 \pm 0.004 \pm 0.008\,. \tag{76.20}$$

We first turn to $|V_{cb}|$ extractions that rely on only the normalization $\mathcal{G}(1)$ from Eq. (76.20). The most precise measurements of $\bar{B} \to D\ell\bar{\nu}_\ell$ [60, 68, 69] dominate the CLN average [6] value, $\eta_{\rm EW}\mathcal{G}(1)|V_{cb}| = (41.53 \pm 0.98) \times 10^{-3}$. Note that this average corresponds to measurements that are fit to the CLN form factor parameterization; the same concerns expressed above for $\bar{B} \to D^*\ell\bar{\nu}_\ell$ apply here. Using the value from Eq. (76.20) for $\mathcal{G}(1)$ and accounting for the electroweak correction as above gives

$$|V_{cb}| = (39.1 \pm 0.9 \pm 0.4) \times 10^{-3} \quad (\bar{B} \to D\ell\bar{\nu}_\ell,\ \text{LQCD, CLN}), \tag{76.21}$$

where the first uncertainty is from experiment, and the second combines the lattice QCD uncertainty in Eq. (76.20) with the electroweak correction.

For the $\bar{B} \to D\ell\bar{\nu}_\ell$ modes, theoretical input on the shape of the form factor, especially near $w \sim 1$, is especially beneficial to $|V_{cb}|$ determinations, since experimental measurements of the differential decays rate near zero recoil are affected by the more severe phase space suppression, compared to the D^* case. Hence the best $|V_{cb}|$ determinations from exclusive $\bar{B} \to D\ell\bar{\nu}_\ell$ decays employ lattice-QCD form factors obtained over a range of $w \geq 1$ [7, 8], where Ref. [70] provides a lattice average of the two results. Using the BCL parametrization (z-expansion from Ref. [71]) for the form factors, they can be combined with binned measurements from Belle [69] and BABAR [68]. Only Ref. [69] published the full measurement covariance matrix, while Ref. [68] provides the statistical uncertainty covariance. Nevertheless, Ref. [69] is more precise and dominates the average [70], giving

$$|V_{cb}| = (40.1 \pm 1.0) \times 10^{-3} \quad (\bar{B} \to D\ell\bar{\nu}_\ell,\ \text{LQCD, BCL}). \tag{76.22}$$

This result is consistent with the value reported in Ref. [47], which is based on the same experimental and lattice inputs.

The $|V_{cb}|$ averages from $\bar{B} \to D^*\ell\bar{\nu}_\ell$ and $\bar{B} \to D\ell\bar{\nu}_\ell$ decays using the BGL (Eq. (76.15)) and BCL (Eq. (76.22)) forms, respectively, are reasonably consistent. The correlations between the lattice uncertainties for $\bar{B} \to D^*\ell\bar{\nu}_\ell$ and $\bar{B} \to D\ell\bar{\nu}_\ell$ are discussed in Ref. [36], and considered to be 100% for the statistical uncertainty component. We assume an experimental uncertainty correlation of order 20% and combine the results of Eq. (76.15) and Eq. (76.22), giving

$$|V_{cb}| = (39.8 \pm 0.6) \times 10^{-3} \quad \text{(exclusive)}. \tag{76.23}$$

76.2.4 $B_s \to D_s^{(*)-}\mu^+\nu_\mu$

Semileptonic decays of B_s mesons are being studied extensively by the LHCb experiment. On the theory side, lattice QCD calculations of the corresponding form factors can proceed using the same methods and gauge-field ensembles as for B-meson decays. In fact, the presence of a strange spectator quark in the B_s-meson decay amplitudes tends to yield smaller statistical and systematic errors in the lattice computation. Nevertheless, to-date there are still fewer lattice-QCD results for B_s-meson form factors available than for the B-meson case, but this situation is expected to change. For the case of the $B_s \to D_s$ transition, two lattice QCD calculations of the form factors

over a range of recoil momenta have been performed by the HPQCD collaboration, the first on 2+1-flavor gauge field ensembles (generated by the MILC collaboration) using NRQCD b-quarks [72]. The second calculation uses the $2+1+1$-flavor gauge-field ensembles (also generated by MILC), employing the HISQ action for all valence quarks [73]. The all-HISQ approach avoids the need to compute renormalization factors separately, at the cost of requiring an extrapolation to the physical b-quark mass at the lattice spacings used in Ref. [73]. For the $B_s \to D_s^{*-}$ transition, Refs. [35, 74] provide lattice QCD results for the form factor at zero recoil, where Ref. [74] uses a similar set-up as Ref. [73] and reads

$$\mathcal{F}^{B_s\to D_s^*}(1) = 0.9020(96)_{\rm stat}(90)_{\rm sys}\,. \tag{76.24}$$

A lattice QCD calculation of the $B_s \to D_s^{*-}$ form factors at non-zero recoil, employing 2+1+1-flavor gauge-field ensembles (generated by MILC) in an all-HISQ approach was presented in Ref. [12] and updated in Ref. [10].

LHCb has extracted $|V_{cb}|$ from semileptonic B_s^0 decays [75]. The measurement uses both $B_s^0 \to D_s^-\mu^+\nu_\mu$ and $B_s^0 \to D_s^{*-}\mu^+\nu_\mu$ decays. The value of $|V_{cb}|$ is determined from the observed yields of B_s^0 decays normalized to those of B^0 decays after correcting for the relative reconstruction and selection efficiencies. The normalization channels are $B^0 \to D^-\mu^+\nu_\mu$ and $B^0 \to D^{*-}\mu^+\nu_\mu$ decays, where the D^- is reconstructed with the same decay mode of the D_s ($D^-_{(s)} \to [K^+K^-]_\phi\pi^-$). The shape of the form factors are extracted using $p_\perp(D_s)$, which is the component of the D_s^- momentum perpendicular to the B_s^0 flight direction. This variable is correlated with q^2 and the helicity angles in the $B_s^0 \to D_s^{*-}\mu^+\nu_\mu$ decay. For the $B_s \to D_s^-\mu^+\nu_\mu$ decay, for example, $|V_{cb}|$ is related to the measured ratio of signal yields, N_{sig}, and the normalization channel yields, N_{ref}, through the relation

$$\frac{N_{sig}}{N_{ref}} = \xi\frac{f_s}{f_d}\frac{\mathcal{B}(D_s^-\to K^+K^-\pi^-)}{\mathcal{B}(D^-\to K^+K^-\pi^-)}\frac{1}{\mathcal{B}(B^0\to D^-\mu\nu_\mu)}\tau_s\int\frac{d\Gamma(B_s\to D_s\mu\nu_\mu)}{dw}dw\ ,$$

where τ_s is the B_s lifetime, and ξ is the efficiency ratio between the signal and the normalization. The analysis uses the lattice-QCD form factors obtained for $B_s \to D_s^-$ over the full kinematic range in Ref. [73] and the zero-recoil result for the $B_s \to D_s^{*-}$ form factor from Ref. [74]. Fits to both the CLN parameterization and a 5-parameter version of BGL were performed. The result for $|V_{cb}|$, updated with the most recent determination of f_s/f_d and $\mathcal{B}(D_s^- \to K^-K^+\pi^-)$ from Ref. [76], are $|V_{cb}|_{\rm CLN} = (40.8 \pm 0.6 \pm 0.9 \pm 1.1) \times 10^{-3}$, and $|V_{cb}|_{\rm BGL} = (41.7 \pm 0.8 \pm 0.9 \pm 1.1) \times 10^{-3}$, where the first uncertainty is statistical, the second systematic and the third due to the limited knowledge of the external inputs, in particular the constant $f_s/f_d \times \mathcal{B}(D_s^- \to K^+K^-\pi^-)$. The determination of $|V_{cb}|$ in Ref. [12], using the lattice form factors obtained therein combined with LHCb data yields a consistent result, $|V_{cb}| = 42.7(1.5)_{\rm latt}(1.7)_{\rm exp}(0.4)_{\rm EM} \times 10^{-3}$. The results obtained are consistent with the exclusive determinations of $|V_{cb}|$ using the B^0 and B^+ decays but are not used in the overall average in this review at this stage. These channels are important in the measurement of the ratio $|V_{ub}|/|V_{cb}|$, which cancels out the B_s normalisation uncertainties, discussed in Section 76.5. LHCb also perform measurements of the $B_s^0 \to D_s^{*-}\mu^+\nu_\mu$ differential decay rate [77]. Fits are performed to extract the form factors in CLN and BGL parametrizations.

76.2.5 $|V_{cb}|$ from inclusive decays

Measurements of the total semileptonic branching decay rate, along with moments of the lepton energy and hadronic invariant mass spectra in inclusive semileptonic $b \to c$ transitions, can be used for a precision determination of $|V_{cb}|$. The total semileptonic decay rate can be calculated quite reliably in terms of non-perturbative parameters that can be extracted from the information contained in the moments.

76.2.6 *Inclusive semileptonic rate*

The theoretical foundation for the calculation of the total semileptonic rate is the Operator Product Expansion (OPE) which yields the Heavy Quark Expansion (HQE) [78, 79]. Details can be found in the RPP mini-review on Effective Theories [3].

The OPE result for the total rate can be written schematically (details can be found, *e.g.*, in Ref. [80]) as

$$\begin{aligned}\Gamma =& |V_{cb}|^2 \frac{G_F^2 m_b^5(\mu)}{192\pi^3} |\eta_{\rm EW}|^2 \times \\ & \left[z_0^{(0)}(r) + \frac{\alpha_s(\mu)}{\pi} z_0^{(1)}(r) + \left(\frac{\alpha_s(\mu)}{\pi}\right)^2 z_0^{(2)}(r) + \cdots \right. \\ & + \frac{\mu_\pi^2}{m_b^2}\left(z_2^{(0)}(r) + \frac{\alpha_s(\mu)}{\pi} z_2^{(1)}(r) + \cdots \right) \\ & + \frac{\mu_G^2}{m_b^2}\left(y_2^{(0)}(r) + \frac{\alpha_s(\mu)}{\pi} y_2^{(1)}(r) + \cdots \right) \\ & + \frac{\rho_{\rm D}^3}{m_b^3}\left(z_3^{(0)}(r) + \frac{\alpha_s(\mu)}{\pi} z_3^{(1)}(r) + \cdots \right) \\ & \left. + \frac{\rho_{\rm LS}^3}{m_b^3}\left(y_3^{(0)}(r) + \frac{\alpha_s(\mu)}{\pi} y_3^{(1)}(r) + \cdots \right) + ... \right] \end{aligned} \tag{76.25}$$

where r is the ratio m_c/m_b and the y_i and z_i are perturbatively calculable Wilson coefficients functions that appear at different orders of the heavy mass expansion.

The parameters μ_π^2, μ_G^2, ρ_D^3 and ρ_{LS}^3 constitute the non-perturbative input into the heavy quark expansion; they correspond to certain matrix elements to be discussed below. In the same way the HQE can be set up for the moments of distributions of charged-lepton energy, hadronic invariant mass and hadronic energy, e.g.

$$\langle E_e^n \rangle_{E_e > E_{\rm cut}} = \int_{E_{\rm cut}}^{E_{\rm max}} \frac{d\Gamma}{dE_e} E_e^n dE_e \Big/ \int_{E_{\rm cut}}^{E_{\rm max}} \frac{d\Gamma}{dE_e} dE_e \, . \tag{76.26}$$

The coefficients of the HQE are known up to order $1/m_b^5$ at tree level [81–84]. The leading term $z_0^{(i)}$ is the parton model, and is known completely through order α_s^2 [85–87] and now also at α_s^3 [88]. The terms of order $\alpha_s^{n+1}\beta_0^n$ (where β_0 is the first coefficient of the QCD β function, $\beta_0 = (33 - 2n_f)/3$) have been included following the BLM procedure [80, 89–92]. Corrections of order $\alpha_s \mu_\pi^2/m_b^2$ have been computed in Ref. [93] and Ref. [94], while the $\alpha_s \mu_G^2/m_b^2$ terms have been calculated in Ref. [95] and Ref. [96], and the $\alpha_s \rho_D^3/m_b^3$ corrections in Refs. [97, 98].

Starting at order $1/m_b^3$ contributions with an infrared sensitivity to the charm mass, m_c, appear [81, 83, 99, 100]. At order $1/m_b^3$ this "intrinsic charm" contribution manifests as a $\log(m_c)$ in the coefficient of the Darwin term ρ_D^3. At higher orders, terms such as $1/m_b^3 \times 1/m_c^2$ and $\alpha_s(m_c) 1/m_b^3 \times 1/m_c$ appear; numerically these terms may be comparable in size to the contributions of order $1/m_b^4$.

The HQE parameters are given in terms of forward matrix elements of local operators; the parameters entering the expansion for orders up to $1/m_b^3$ are ($D_\perp^\mu = (g_{\mu\nu} - v_\mu v_\nu) D^\nu$, where $v =$

p_B/M_B is the four-velocity of the B meson)

$$\begin{aligned}
\overline{\Lambda} &= M_B - m_b\,, \\
\mu_\pi^2 &= -\langle B|\bar{b}(iD_\perp)^2 b|B\rangle\,, \\
\mu_G^2 &= \langle B|\bar{b}(iD_\perp^\mu)(iD_\perp^\nu)\sigma_{\mu\nu} b|B\rangle\,, \\
\rho_{\rm D}^3 &= \langle B|\bar{b}(iD_{\perp\mu})(ivD)(iD_\perp^\mu) b|B\rangle\,, \\
\rho_{\rm LS}^3 &= \langle B|\bar{b}(iD_\perp^\mu)(ivD)(iD_\perp^\nu)\sigma_{\mu\nu} b|B\rangle. \qquad (76.27)
\end{aligned}$$

These parameters still depend on the heavy quark mass. Sometimes the infinite mass limits of these parameters $\overline{\Lambda} \to \overline{\Lambda}_{\rm HQET}$, $\mu_\pi^2 \to -\lambda_1$, $\mu_G^2 \to 3\lambda_2$, $\rho_D^3 \to \rho_1$ and $\rho_{LS}^3 \to 3\rho_2$, are used instead. Beyond $1/m^3$ the number of independent HQE parameters starts to proliferate [84,101]. In general, there are 13 parameters (at tree level) up to order $1/m^4$ and 31 (at tree level) up to order $1/m^5$, not including $\overline{\Lambda}$. A framework to compute observables at higher order in $1/m$ [84, 102] has been used to estimate the HQE parameters of the orders $1/m_b^4$ and $1/m_b^5$. Their their impact on the $|V_{cb}|$ determination has been studied in Ref. [103]. However, as pointed out in Ref. [104] one may reduce the number of independent parameters in the HQE by exploiting reparametrization invariance, which is a symmetry of the HQE stemming from Lorentz invariance of QCD. For a subset of observables this allows us to reduce the number of parameters to three up to order $1/m^3$ (ρ_{LS}^3 can be absorbed into μ_G^2 by a re-definition) and to 8 up to order $1/m^4$ [105].

The perturbative QCD expansion for the decay rate does not converge, in general. In addition, the expansion coefficients in the rates and spectra depend strongly on the scheme used for m_b (or equivalently on $\overline{\Lambda}$). It is well known (see eg. [106]) that using the pole mass definition for heavy quark masses leads to particularly badly behaved expansions. This motivates the use of "short-distance" mass definitions, such as the kinetic scheme [37] or the $1S$ scheme [107–109]. Both schemes are well suited for the HQE, since they allow the choice of the renormalization scale $\mu \leq m_b$. Furthermore, in both schemes, the masses can be extracted from other observables with sufficient precision, enabling a precise determination of $|V_{cb}|$, despite of the strong quark-mass dependence of the total rate.

The $1S$ scheme eliminates the b quark pole mass by relating it to the perturbative expression for the mass of the $1S$ state of the Υ system. The b quark mass in the $1S$ scheme is half of the perturbatively calculated mass of the $1S$ state of the Υ system. The best determination of the b quark mass in the $1S$ scheme is obtained from sum rules for $e^+e^- \to b\bar{b}$ [110]. A second alternative is the so-called "kinetic mass" $m_b^{\rm kin}(\mu)$, which enters the non-relativistic expression for the kinetic energy of a heavy quark, and is defined using heavy-quark sum rules [37]. The relation between $m_b^{\rm kin}$ and $m_b^{\overline{MS}}$ is known through three-loop order [111].

Finally, we note that the theoretical description of inclusive decays employed here, is based on the assumption of quark-hadron duality. While there is no evidence of violations of quark-hadron duality, the theoretical uncertainties due to such violations are not well quantified [3].

76.2.7 *Determination of HQE Parameters and $|V_{cb}|$*

Several experiments have measured moments in $\bar{B} \to X_c \ell \bar{\nu}_\ell$ decays [112–120] as a function of the minimum lepton momentum. Recently, moments measurements have been performed as a function of lepton invariant mass squared, q^2 [121, 122]. The measurements of the moments of the electron energy spectrum ($0^{\rm th}$-$3^{\rm rd}$) and of the squared hadronic mass spectrum ($0^{\rm th}$-$2^{\rm nd}$) have statistical uncertainties that are roughly equal to their systematic uncertainties. The $3^{\rm rd}$ order hadronic mass spectrum moments have also been measured by some experiments, with relatively large statistical uncertainty. The sets of moments measured within each experiment have strong correlations; their

use in a global fit requires fully specified statistical and systematic covariance matrices. Measurements of photon energy moments (0^{th}-2^{nd}) in $B \to X_s\gamma$ decays [123–127] as a function of the minimum accepted photon energy are also used in some fits; the dominant uncertainties on these measurements are statistical.

Global fits [120, 124, 128–134] to the moments of the electron energy spectrum and the squared hadronic mass spectrum have been performed in the $1S$ and kinetic schemes. The semileptonic moments alone determine a linear combination of m_b and m_c very accurately but leave the orthogonal combination poorly determined (See e.g. [135]); additional input is required to allow a precise determination of m_b. This additional information can come from the radiative $B \to X_s\gamma$ moments (with the caveat that the OPE for $b \to s\gamma$ breaks down beyond leading order in $\Lambda_{\rm QCD}/m_b$), which provide complementary information on m_b and μ_π^2, or from precise determinations of the charm and beauty quark masses [36, 70, 136]. The values obtained in the kinetic scheme fits [6, 132, 133] with these two constraints are consistent. Based on the charm and beauty quark mass constraints [36, 134] $m_c^{\overline{\rm MS}}(3\,{\rm GeV}) = 0.988 \pm 0.007\,{\rm GeV}$, and $m_b^{\overline{\rm MS}} = 4.198 \pm 0.012){\rm GeV}$ a fit in the kinetic scheme [134] obtains

$$|V_{cb}| = (42.16 \pm 0.51) \times 10^{-3} \tag{76.28}$$

where the error include experimental and theoretical uncertainties. This analysis [134] includes calculations of the third-order corrections to the semi-leptonic $b \to c\ell\nu$ decay width [88] and mass relations [111,137] Theoretical uncertainties from higher orders in $1/m$ as well as in α_s are estimated and included in performing the fits. Similar values for the parameters are obtained with a variety of assumptions about the theoretical uncertainties and their correlations. The χ^2/dof is well below unity, which could suggest that the theoretical uncertainties may be overestimated. However, while one could obtain a satisfactory fit with smaller uncertainties, this would result in unrealistically small uncertainties on the extracted HQE parameters, which are used as input to other calculations (e.g. the determination of $|V_{ub}|$).

A fit to the measured moments in the $1S$ scheme [6, 124, 131] gives

$$|V_{cb}| = (41.98 \pm 0.45) \times 10^{-3}, \tag{76.29}$$

$$m_b^{1S} = (4.691 \pm 0.037)\,{\rm GeV}. \tag{76.30}$$

This fit uses moments measurements from semileptonic and radiative decays and constrains the chromomagnetic operator using the B^*-B and D^*-D mass differences, but does not include the constraint on m_c nor all known higher order corrections.

Measurements of higher order moments and moments of additional variables, such as q^2, can further improve the sensitivity of the fits to higher-order terms in the HQE [105]. The q^2 moments depend on a reduced set of operators, thereby possibly making it easier to extract higher-order terms from data. A fit to the q^2 moments measured by the Belle [121] and Belle II [122] experiments combined with the world average inclusive branching fractions, finds [138]:

$$|V_{cb}| = (41.69 \pm 0.63) \times 10^{-3}\ , \tag{76.31}$$

which is compatible with the fit to the other moments. Note there is a strong correlation with the other determinations due to the use of common inputs for the branching fractions.

These fits give consistent results for $|V_{cb}|$ and, after translation to a common renormalization scheme, for m_b. We take the fit in the kinetic scheme [134], which includes higher-order perturbative corrections, as the inclusive determination of $|V_{cb}|$:

$$|V_{cb}| = (42.2 \pm 0.5) \times 10^{-3}\ \text{(inclusive)}. \tag{76.32}$$

76.3 Determination of $|V_{ub}|$

Summary: Currently the best determinations of $|V_{ub}|$ are from $\bar{B} \to \pi \ell \bar{\nu}_\ell$ decays, where combined fits to theory and experimental data as a function of q^2 provide a precision of about 4%; the uncertainties from experiment and theory are comparable in size. Determinations based on inclusive semileptonic B decays are based on different observables and use different strategies to suppress the $b \to c$ background. Most of the determinations are consistent and provide a precision of about 7%, with comparable contributions to the uncertainty from experiment and theory.

The values obtained from inclusive and exclusive B decay determinations are

$$|V_{ub}| = (4.13 \pm 0.12 \,^{+\,0.13}_{-\,0.14} \pm 0.18) \times 10^{-3} \quad \text{(inclusive)}, \tag{76.33}$$

$$|V_{ub}| = (3.70 \pm 0.10 \pm 0.12) \times 10^{-3} \quad \text{(exclusive)}, \tag{76.34}$$

where the last uncertainty on the inclusive result was added by the authors of this review and is discussed below. The exclusive and inclusive determinations are independent, and the dominant uncertainties are on multiplicative factors. The results from the two determinations are compatible to within two standard deviations.

This can be compared to the values derived from $|V_{ub}|/|V_{cb}|$ ratio measurements, described in the next section. Taking the value for this ratio from Eq. (76.54), and $|V_{cb}|$ from Eq. (76.3) we obtain.

$$|V_{ub}| = (3.43 \pm 0.32) \times 10^{-3} \qquad (\mathrm{B_s},\ \Lambda_\mathrm{b}), \tag{76.35}$$

We choose to combine only the direct determinations of $|V_{ub}|$, based on the inclusive and exclusive B measurements. In the combination they are weighted by their relative errors, where the uncertainties are treated as normally distributed. The resulting average has $p(\chi^2) = 15\%$, so we scale the error by $\sqrt{\chi^2/1} = 1.4$ to find

$$|V_{ub}| = (3.82 \pm 0.20) \times 10^{-3} \quad \text{(average)}. \tag{76.36}$$

In a future update we may consider the constraints in the $|V_{ub}|$-$|V_{cb}|$ plane from the direct determinations together with the LHCb $|V_{ub}/V_{cb}|$ results, although the agreement among all inputs is somewhat marginal.

76.3.1 $|V_{ub}|$ *from inclusive decays*

The theoretical description of inclusive $\bar{B} \to X_u \ell \bar{\nu}_\ell$ decays is based on the Heavy Quark Expansion and leads to a predicted total decay rate with uncertainties below 5% [108,139]. However, the total decay rate is hard to measure due to the large background from CKM-favored $\bar{B} \to X_c \ell \bar{\nu}_\ell$ transitions, and hence the theoretical methods differ from the $\bar{B} \to X_c \ell \bar{\nu}_\ell$ case. For a calculation of the partial decay rate in regions of phase space where $\bar{B} \to X_c \ell \bar{\nu}_\ell$ decays are suppressed one cannot use the HQE as for $b \to c$, rather one needs to introduce non-perturbative distribution functions, the "shape functions" (SF) [140,141]. Their exact form is not known, but its moments can be related to the HQE parameters known e.g from the $b \to c$ case.

The shape functions become important when the light-cone momentum component $P_+ \equiv E_X - |P_X|$ is not large compared to Λ_{QCD}, as is the case near the endpoint of the $\bar{B} \to X_u \ell \bar{\nu}_\ell$ lepton spectrum. Partial rates for $\bar{B} \to X_u \ell \bar{\nu}_\ell$ are predicted and measured in a variety of kinematic regions that differ in their sensitivity to shape-function effects.

At leading order in $1/m_b$ only a single shape function (SF) appears, which is universal for all heavy-to-light transitions [140,141] and can be extracted in $\bar{B} \to X_s \gamma$ decays. At subleading order in $1/m_b$, several shape functions appear [142], along with small "resolved photon contributions"

specific for $\bar{B} \to X_s\gamma$ [143–145], and thus the prescriptions that relate directly the partial rates for $\bar{B} \to X_s\gamma$ and $\bar{B} \to X_u\ell\bar{\nu}_\ell$ decays [146–154] are limited to leading order in $1/m_b$.

Existing approaches use parametrizations of the leading SF that respect constraints on the normalization and on the first and second moments, which are given in terms of the HQE parameters $\overline{\Lambda} = M_B - m_b$ and μ_π^2, respectively. The relations between SF moments and the HQE parameters are known to second order in α_s [155]; as a result, measurements of HQE parameters from global fits to $\bar{B} \to X_c\ell\bar{\nu}_\ell$ and $\bar{B} \to X_s\gamma$ moments can be used to constrain the SF moments, as well as to provide accurate values of m_b and other parameters for use in determining $|V_{ub}|$. Flexible parametrizations of the SF using orthogonal basis functions [156] or artificial neural networks [157] allow global fits to inclusive B meson decay data [145] that incorporate the known short-distance contributions and renormalization properties of the SF.

HFLAV performs fits on the basis of several approaches, with varying degrees of model dependence. We will consider here the approaches documented in Ref. [158] (BLNP), Ref. [159] (GGOU) and Ref. [160] (DGE).

The triple differential rate in the variables

$$P_\ell = M_B - 2E_\ell, \quad P_- = E_X + |\vec{P}_X|, \quad P_+ = E_X - |\vec{P}_X| \tag{76.37}$$

is

$$\begin{aligned} \frac{d^3\Gamma}{dP_+\, dP_-\, dP_\ell} &= \frac{G_F^2|V_{ub}|^2}{16\pi^2}(M_B - P_+) \\ &\Big\{(P_- - P_\ell)(M_B - P_- + P_\ell - P_+)\mathcal{F}_1 \\ &\quad + (M_B - P_-)(P_- - P_+)\mathcal{F}_2 + (P_- - P_\ell)(P_\ell - P_+)\mathcal{F}_3\Big\}. \end{aligned} \tag{76.38}$$

The "structure functions", $\mathcal{F}_i$, can be calculated using factorization theorems that have been proven to subleading order in the $1/m_b$ expansion [161].

The BLNP [158] calculation uses these factorization theorems to write the $\mathcal{F}_i$ terms as functions of perturbatively calculable hard coefficients and jet functions, which are convolved with the (soft) light-cone distribution functions.The calculation of $\mathcal{O}(\alpha_s^2)$ contributions [162, 163] is not yet complete and is not included in the $|V_{ub}|$ determination given below.

The leading order term in the $1/m_b$ expansion of the $\mathcal{F}_i$ terms contains a single non-perturbative function and is calculated to subleading order in α_s, while at subleading order in the $1/m_b$ expansion there are several independent non-perturbative functions that have been calculated only at tree level in the α_s expansion.

A distinct approach (GGOU) [159] uses a hard, Wilsonian cut-off that matches the definition of the kinetic mass. The non-perturbative input is similar to what is used in BLNP, but the shape functions are defined differently. In particular, they are defined at finite m_b and depend on the light-cone component k_+ of the b quark momentum and on the momentum transfer q^2 to the leptons. These functions include subleading effects to all orders; as a result they are non-universal, with one shape function corresponding to each structure function in Eq. (76.38). Their k_+ moments can be computed in the OPE.

Going to subleading order in α_s requires the definition of a renormalization scheme for the HQE parameters and for the SF. The relation between the moments of the SF and the forward matrix elements of local operators appearing the HQE is plagued by ultraviolet problems and requires additional renormalization. A scheme for improving this behavior was suggested in Refs. [158, 164], which introduce a definition of the quark mass (the so-called shape-function scheme) based on the

first moment of the measured $\bar{B} \to X_s\gamma$ photon energy spectrum. Likewise, the HQE parameters can be defined from measured moments of spectra, corresponding to moments of the SF.

There are various ideas to model the SF, but this requires additional assumptions. One approach (DGE) is the so-called "dressed gluon exponentiation" [160], where the perturbative result is continued into the infrared regime using the renormalon structure obtained in the large β_0 limit, where β_0 has been defined following Eq. (76.25). Other approaches make even stronger assumptions, such as in Ref. [165], which assumes an analytic behavior for the strong coupling in the infrared to perform an extrapolation of perturbation theory.

In order to reduce sensitivity to SF uncertainties, measurements that use a combination of cuts on the leptonic momentum transfer q^2 and the hadronic invariant mass m_X, as suggested in Ref. [166,167], have been made. In general, experimental measurements of $\bar{B} \to X_u\ell\bar{\nu}_\ell$ into charm-dominated regions (in order to reduce SF uncertainties) are sensitive to the modeling of $\bar{B} \to X_u\ell\bar{\nu}_\ell$ and $\bar{B} \to X_c\ell\bar{\nu}_\ell$ decays. The measurements quoted below have used a variety of functional forms to parametrize the leading SF; a specific error budget for one determination is quoted in the next section. In no case is the parametrization uncertainty estimated to be more than a 2% on $|V_{ub}|$.

Weak Annihilation [159,168,169] (WA) can in principle contribute significantly in the high-q^2 region of $\bar{B} \to X_u\ell\bar{\nu}_\ell$ decays. Estimates based on semileptonic D_s decays [100,166,167,169] lead to a $\sim 2\%$ uncertainty on the total $\bar{B} \to X_u\ell\bar{\nu}_\ell$ rate from the $\Upsilon(4S)$. The q^2 spectrum of the WA contribution is not well known, but from the OPE it is expected to contribute predominantly at high q^2. Other theoretical investigations [100,170,171], a direct search [172], and $\mathcal{B}(B^0 \to X_u\ell\bar{\nu})/\mathcal{B}(B^+ \to X_u\ell\bar{\nu})$ ratio measurements [173–176] indicate that WA is a small effect, but may become a significant source of uncertainty for $|V_{ub}|$ measurements that accept only a small fraction of the full $\bar{B} \to X_u\ell\bar{\nu}_\ell$ phase space.

76.3.2 *Measurements*

We summarize the measurements used in the determination of $|V_{ub}|$ below. Given the improved precision and more rigorous theoretical interpretation of more recent measurements, determinations [177–180] done with LEP data are not considered in this review.

Inclusive electron momentum measurements [181,182] reconstruct a single charged electron to determine a partial decay rate for $\bar{B} \to X_u\ell\bar{\nu}_\ell$ near the kinematic endpoint. This results in a selection efficiency of order 50% and only modest sensitivity to the modeling of detector response. The inclusive electron momentum spectrum from $B\bar{B}$ events, after subtraction of the $e^+e^- \to q\bar{q}$ continuum background, is fitted to a model $\bar{B} \to X_u\ell\bar{\nu}_\ell$ spectrum and several components ($D\ell\bar{\nu}_\ell$, $D^*\ell\bar{\nu}_\ell$, ...) of the $\bar{B} \to X_c\ell\bar{\nu}_\ell$ background; the dominant uncertainties are related to this subtraction and modelling. The decay rate can be cleanly extracted for $E_e > 2.3\,\text{GeV}$, but this is deep in the SF region, where theoretical uncertainties are large. More recent measurements have increased the accessed phase phase. The resulting $|V_{ub}|$ values for various E_e cuts are given in Table 76.2.

The most recent BABAR measurement [183] is based on the inclusive electron spectrum and determines the partial branching fraction and $|V_{ub}|$ for $E_e > 0.8\,\text{GeV}$. The analysis shows that the partial branching fraction measurements can have signal model dependence when the kinematic acceptance includes regions dominated by $\bar{B} \to X_c\ell\bar{\nu}_\ell$ background. The model dependence enters primarily through the partial branching fractions, and arises because the signal yield fit has sensitivity to $\bar{B} \to X_u\ell\bar{\nu}_\ell$ decays only in regions with good signal to noise.

An untagged "neutrino reconstruction" measurement [184] from BABAR uses a combination [185] of a high-energy electron with a measurement of the missing momentum vector. This allows S/B~ 0.7 for $E_e > 2.0\,\text{GeV}$ and a $\approx 5\%$ selection efficiency, but at the cost of a smaller accepted phase space for $\bar{B} \to X_u\ell\bar{\nu}_\ell$ decays and uncertainties associated with the determination of the missing momentum.

The large samples accumulated at the B factories allow studies in which one B meson is fully reconstructed and the recoiling B decays semileptonically [186–189]. The experiments can fully reconstruct a "tag" B candidate in about 0.5% (0.3%) of B^+B^- ($B^0\bar{B}^0$) events. An electron or muon with center-of-mass momentum above 1.0 GeV is required amongst the charged tracks not assigned to the tag B and the remaining particles are assigned to the X_u system. The full set of kinematic properties (E_ℓ, m_X, q^2, *etc.*) are available for studying the semileptonically decaying B, making possible selections that accept up to 90% of the full $\bar{B} \to X_u \ell \bar{\nu}_\ell$ rate; however, the sensitivity to $\bar{B} \to X_u \ell \bar{\nu}_\ell$ decays is still driven by the regions where $\bar{B} \to X_c \ell \bar{\nu}_\ell$ decays are suppressed. Despite requirements (e.g. on the square of the missing mass) aimed at rejecting events with additional missing particles, undetected or mis-measured particles from $\bar{B} \to X_c \ell \bar{\nu}_\ell$ decay (e.g., K_L^0 and additional neutrinos) remain an important source of uncertainty.

A recent recoil method measurement of partial branching fractions in three phase-space regions, covering about 31% to 86% of the accessible phase space, was performed by Belle [173], where machine learning techniques were used to reduce background levels. The measurement contains substantial decay model updates and supersedes previous measurements from Belle [187,188]. The measurement of the partial branching fraction obtained in the $E_\ell^B > 1$GeV region, the most precise one, is used to obtain $|V_{ub}|$ [173]. Belle also reports measurements of the background subtracted, and unfolded differential decay spectra in bins of m_X, m_X and q^2, P_+ and E_ℓ [190] for use in global fit analyses.

Earlier measurements by BABAR [186] were also performed with cuts on m_X, m_X and q^2, P_+ and E_ℓ using the recoil method. In each case the experimental systematic uncertainties have significant contributions from the modeling of $\bar{B} \to X_u \ell \bar{\nu}_\ell$ and $\bar{B} \to X_c \ell \bar{\nu}_\ell$ decays and from the detector response to charged particles, photons and neutral hadrons.

To reduce modelling uncertainties associated to $\bar{B} \to X_c \ell \bar{\nu}_\ell$ decays a recent Belle tagged measurement [176] uses a novel data driven approach to correct the kinematics and normalisation of this background component, while using less restrictive event selection with higher efficiency than the other recent Belle result. In the analysis the ratio $|V_{ub}|/|V_{cb}|$ is directly extracted from inclusive decays for the first time. While a value for $|V_{ub}|$ is provided here, it is not yet included in the combination.

The corresponding $|V_{ub}|$ values are given in Table 76.2.

76.3.3 $|V_{ub}|$ *from inclusive partial rates*

The measured partial rates and theoretical calculations from BLNP, GGOU and DGE described previously are used to determine $|V_{ub}|$ from all measured partial $\bar{B} \to X_u \ell \bar{\nu}_\ell$ rates [6]; selected values are given in Table 76.2. The correlations amongst the multiple BABAR recoil-based measurements [186] are fully accounted for in the average. The statistical correlations amongst the other measurements used in the average are small (due to small overlaps among signal events and large differences in S/B ratios) and have been ignored. Correlated systematic and theoretical errors are taken into account, both within an experiment and between experiments. As an illustration of the relative sizes of the uncertainties entering $|V_{ub}|$ we give the error breakdown for the GGOU average: statistical—1.3%; experimental—1.6%; $\bar{B} \to X_c \ell \bar{\nu}_\ell$ modeling—0.9%; $\bar{B} \to X_u \ell \bar{\nu}_\ell$ modeling—1.7%; HQE parameters (m_b) —1.8%; higher-order corrections—1.5%; q^2 modeling—1.3%; Weak Annihilation—$^{+0.0}_{-1.1}$%; SF parametrization—0.1%.

The averages quoted here are based on the following m_b values: $m_b^{SF} = 4.582 \pm 0.023 \pm 0.018$ GeV for BLNP, $m_b^{\rm kin} = 4.554 \pm 0.018$ GeV for GGOU, and $m_b^{\overline{MS}} = 4.188 \pm 0.043$ GeV for DGE. The $m_b^{\rm kin}$ value is determined in a global fit to moments in the kinetic scheme [6]; this value is translated into m_b^{SF} and $m_b^{\overline{MS}}$ at fixed order in α_s. The second uncertainty quoted on m_b arises from the scheme translation.

Table 76.2: $|V_{ub}|$ (in units of 10^{-5}) from inclusive $\bar{B} \to X_u \ell \bar{\nu}_\ell$ measurements. The first uncertainty on $|V_{ub}|$ is experimental, while the second includes both theoretical and HQE parameter uncertainties. The values are generally listed in order of increasing kinematic acceptance, f_u (0.19 to 0.90), except for the BABAR E_e >0.8 GeV measurement; those below the horizontal bar are based on recoil methods. The Belle 2023 measurement is not yet included in the combination.

Ref.	cut (GeV)	BLNP	GGOU	DGE
CLEO [181]	$E_e > 2.1$	$422 \pm 49 \,^{+\,29}_{-\,34}$	$423 \pm 49 \,^{+\,22}_{-\,31}$	$386 \pm 45 \,^{+\,25}_{-\,27}$
BABAR [184]	$E_e - q^2$	$471 \pm 32 \,^{+\,33}_{-\,38}$	not available	$435 \pm 29 \,^{+\,28}_{-\,30}$
Belle [182]	$E_e > 1.9$	$493 \pm 46 \,^{+\,26}_{-\,29}$	$495 \pm 46 \,^{+\,16}_{-\,21}$	$482 \pm 45 \,^{+\,23}_{-\,23}$
BABAR [183]	$E_e > 0.8$	$441 \pm 12 \,^{+\,27}_{-\,27}$	$396 \pm 10 \,^{+\,17}_{-\,17}$	$385 \pm 11 \,^{+\,8}_{-\,7}$
BABAR [186]	$^{q^2>8}_{m_X<1.7}$	$432 \pm 23 \,^{+\,26}_{-\,28}$	$433 \pm 23 \,^{+\,24}_{-\,27}$	$424 \pm 22 \,^{+\,18}_{-\,21}$
BABAR [186]	$P_+ < 0.66$	$409 \pm 25 \,^{+\,25}_{-\,25}$	$425 \pm 26 \,^{+\,26}_{-\,27}$	$417 \pm 25 \,^{+\,28}_{-\,37}$
BABAR [186]	$m_X < 1.7$	$403 \pm 22 \,^{+\,22}_{-\,22}$	$410 \pm 23 \,^{+\,16}_{-\,17}$	$422 \pm 23 \,^{+\,21}_{-\,27}$
BABAR [186]	$E_\ell > 1.3$	$433 \pm 24 \,^{+\,19}_{-\,21}$	$444 \pm 24 \,^{+\,9}_{-\,10}$	$445 \pm 24 \,^{+\,12}_{-\,13}$
Belle [173]	$E_\ell > 1$	$405 \pm 23 \,^{+\,18}_{-\,20}$	$415 \pm 24 \,^{+\,8}_{-\,9}$	$416 \pm 24 \,^{+\,11}_{-\,12}$
Belle [176]	$E_\ell > 1$	$415 \pm 24 \,^{+\,18}_{-\,20}$	$425 \pm 25 \,^{+\,8}_{-\,9}$	$426 \pm 25 \,^{+\,11}_{-\,12}$
HFLAV [6]	Combination	$428 \pm 13 \,^{+\,20}_{-\,21}$	$419 \pm 12 \,^{+\,11}_{-\,12}$	$392 \pm 10 \,^{+\,9}_{-\,10}$

Hadronization uncertainties also impact the $|V_{ub}|$ determination. The theoretical expressions are valid at the parton level and do not incorporate any resonant structure (*e.g.* $\bar{B} \to \pi \ell \bar{\nu}_\ell$); this must be added to the simulated $\bar{B} \to X_u \ell \bar{\nu}_\ell$ event samples, since the detailed final state multiplicity and structure impacts the estimates of experimental acceptance and efficiency. The experiments have adopted procedures to input resonant structure while preserving the appropriate behavior in the kinematic variables (q^2, E_ℓ, m_X) averaged over the sample, but these prescriptions are *ad hoc* and ultimately require *in situ* calibration. The resulting uncertainties have been estimated to be $\sim$ 1-2% on $|V_{ub}|$. A recent inclusive $|V_{ub}|$ Belle measurement is the first to perform a fit to final state pion multiplicity for *in situ* calibration of the hadronization models used. The measurement simultaneously extracts inclusive and exclusive $|V_{ub}|$, with compatible results [191].

All calculations yield compatible $|V_{ub}|$ values and similar error estimates. The arithmetic mean of the values and errors of the HFLAV combinations listed in Table 76.2 is $|V_{ub}| = (4.13 \pm 0.12_{\rm exp}\,^{+0.13}_{-0.14\,\rm theo}) \times 10^{-3}$, although there is a spread of approximately 10% in the evaluations with the three theoretical models. For reasons discussed below, we assign an additional uncertainty due to model dependence that is not reflected in the HFLAV averages. As highlighted in the BABAR analysis [173, 183], model dependence entering measurement procedures can be sizeable, and is not consistently treated across analyses. Many of the analyses shown in Table 76.2 were based on partial branching fraction measurements determined in a single model (i.e. the one used by that analysis when simulating $\bar{B} \to X_u \ell \bar{\nu}_\ell$ decays), although in some cases simulated events were weighted to match the expected spectra in other models and the differences introduced as systematic uncertainties, e.g. Ref. [188]. The $|V_{ub}|$ value quoted by HFLAV for each model are, typically, derived from this unique partial branching fraction combined with another model-specific partial rate calculation. The model dependence in the partial branching fraction is sensitive to how the model predictions compare in the restricted region with good signal-to-noise, not by how they compare when integrated over the full kinematic range used in the fit. Ideally this effect needs to be accounted for by the experiments; the published information is insufficient to determine it. To

account for the range in results using the different theoretical models, we take half of the spread of the averages as an additional systematic uncertainty, denoted Δmodel. With this addition, the inclusive $|V_{ub}|$ average is

$$|V_{ub}| = (4.13 \pm 0.12_{\rm exp}\ ^{+0.13}_{-0.14\ \rm theo} \pm 0.18_{\Delta\rm model}) \times 10^{-3} \quad \text{(inclusive)}. \tag{76.39}$$

76.3.4 $|V_{ub}|$ from exclusive decays

Exclusive charmless semileptonic decays offer a complementary means of determining $|V_{ub}|$. For the experiments, the specification of the final state provides better background rejection, but the branching fraction to a specific final state is typically only a few percent of that for inclusive decays. For theory, the calculation of the form factors for decays of B-mesons into exclusive final states is challenging, but brings in a different set of uncertainties from those encountered in inclusive decays. In this review we focus on $\bar{B} \to \pi\ell\bar{\nu}_\ell$, as it is the most promising decay mode for both experiment and theory. However, we also discuss $\bar{B}_s \to K\ell\bar{\nu}_\ell$ decays, for which there are recent interesting results. Measurements of other exclusive $\bar{B} \to X_u\ell\bar{\nu}_\ell$ decays can be found in Refs. [192–205].

76.3.5 $\bar{B} \to \pi\ell\bar{\nu}_\ell$ form factor calculations

The relevant form factors for the decay $\bar{B} \to \pi\ell\bar{\nu}_\ell$ are usually defined as

$$\begin{aligned}&\langle\pi(p_\pi)|V^\mu|B(p_B)\rangle = \\ &f_+(q^2)\left[p_B^\mu + p_\pi^\mu - \frac{m_B^2 - m_\pi^2}{q^2}q^\mu\right] + f_0(q^2)\frac{m_B^2 - m_\pi^2}{q^2}q^\mu\end{aligned} \tag{76.40}$$

in terms of which the rate becomes (in the limit $m_\ell \to 0$)

$$\frac{d\Gamma}{dq^2} = \frac{G_F^2|V_{ub}|^2}{24\pi^3}|p_\pi|^3|f_+(q^2)|^2, \tag{76.41}$$

where p_π is the pion momentum in the B meson rest frame.

Lattice-QCD calculations of the form factors for the $B \to \pi\ell\bar{\nu}$ and $B_s \to K\ell\bar{\nu}$ transitions are available from the Fermilab/MILC [206,207], HPQCD [208], RBC/UKQCD [209,210], and JLQCD [211] collaborations. The lattice form factors are obtained in the large q^2 region, $q^2_{\rm max} > q^2 \gtrsim 15\,{\rm GeV}^2$ and the calculations differ in actions employed for the b quark. While HPQCD [208] is using lattice-nonrelativistic QCD, the results from Fermilab/MILC [206, 207]and RBC/UKQCD [209] are obtained with relativistic b quark actions based on the Fermilab approach [212], albeit using independently generated gauge-field configurations. The JLQCD collaboration is using all-domain-wall-fermion set-up, The results agree within the quoted errors. For the $B \to \pi$ form factor $f_+(q^2 = 20\,{\rm GeV}^2)$, Ref. [206] quotes uncertainty of 3.4%, where the leading contribution is due to the chiral-continuum extrapolation fit, which includes statistical and heavy-quark discretization errors.

The extrapolation to small values of q^2 can be performed using guidance from analyticity and unitarity together with a conformal mapping of the kinematical variables onto the complex unit disc, which yields series in the variable

$$z = \frac{\sqrt{t_+ - q^2} - \sqrt{t_+ - t_0}}{\sqrt{t_+ - q^2} + \sqrt{t_+ - t_0}}\,, \tag{76.42}$$

where $t_\pm = (M_B \pm m_\pi)^2$ and the choice of t_0 determines the range of z that corresponds to the kinematic range of the decay. Setting $t_0 = t_-$ results in $z = 0$ when $q^2 = q^2_{\rm max}$. The choice $t_0 = (m_B + m_\pi)/(\sqrt{m_B} - \sqrt{m_\pi})^2$ centers the kinematic range around $z = 0$, so that $|z| < 0.3$.

We note that the $\bar{B}_s \to K\ell\bar{\nu}_\ell$ decay is an example were the implementation of unitarity bounds is complicated by the fact that the location of the cut in the q^2 plane is different from the B_sK threshold, because the cut starts at $B\pi$ production threshold. Modifications of the unitarity constraints in this and similar examples are discussed in Refs. [210, 213–216].

The "BCL" parameterization of Ref. [71] is commonly used for these decays, as it is consistent with the asymptotic scaling ($q^2 \to \infty$) as well as near threshold, $q^2 = t_+$. As pointed out in Ref. [217] the unitarity sum of the z-expansion coefficients for f_+ is expected to be of order $(\Lambda/m)^3$, hence yielding a rapidly converging series. We note that relatively small differences in different lattice QCD form factor results can be amplified by a long extrapolation to the low-q^2 region. However, such extrapolations are not needed, when lattice form factors are combined with experimental measurements of the differential decay rate. The joint fits provide constraints on the shape of the form factor over the entire kinematic range, in addition to enabling precise determinations of $|V_{ub}|$ [218].

LCSR calculations provide estimates for the product $f_B f_+(q^2)$, valid in the region $0 < q^2 \lesssim 12$ GeV. The determination of $f_+(q^2)$ itself requires knowledge of the decay constant f_B, which is usually obtained by replacing f_B by its two-point QCD (SVZ) sum rule [219] in terms of perturbative and condensate contributions. The advantage of this procedure is the approximate cancellation of various theoretical uncertainties in the ratio $(f_B f_+)/(f_B)$. The LCSR for $f_B f_+$ is based on the light-cone OPE of the relevant vacuum-to-pion correlation function, calculated in full QCD at finite b-quark mass. The resulting expressions comprise a triple expansion: in the twist, t, of the operators near the light-cone, in α_s, and in the deviation of the pion distribution amplitudes from their asymptotic form, which is fixed from conformal symmetry. The state-of-the-art calculations include the leading twists two, three and four with full one-loop α_s corrections [220,221] and partial two-loop corrections [222]. Higher-twist contributions have been investigated in Ref. [223] and two-particle higher twist contributions are studied in Ref. [43]. Nevertheless, estimates based on LCSR generally suffer from difficult to quantify systematic uncertainties.

A detailed statistical analysis including the various correlations has been performed in Ref. [224], also including unitarity bounds on the form factor. The results obtained are numerically compatible with the lattice QCD calculations of the form factor. A more recent analysis [225] employs a modified BCL expansion to extrapolate the LCSR form factors obtained at low q^2 to the high q^2 region, where good agreement with lattice QCD form factor predictions is found. The LCSR form factors can be combined with experimental data in joint z-expansion fits to determine $|V_{ub}|$.

76.3.6 $\bar{B} \to \pi\ell\bar{\nu}_\ell$ measurements

The $\bar{B} \to \pi\ell\bar{\nu}_\ell$ measurements fall into two broad classes: untagged, in which case the reconstruction of the missing momentum of the event serves as an estimator for the unseen neutrino, and tagged, in which the second B meson in the event is fully reconstructed in either a hadronic or semileptonic decay mode. The tagged measurements have better q^2 resolution, high and uniform acceptance and S/B as high as 10, but lower statistical power. The untagged measurements have higher background (S/B < 1) and make slightly more restrictive kinematic cuts, but still provide statistical power precision on the q^2 dependence of the form factor.

CLEO has analyzed $\bar{B} \to \pi\ell\bar{\nu}_\ell$ and $\bar{B} \to \rho\ell\bar{\nu}_\ell$ using an untagged analysis [199–201]. Similar analyses have been done at BABAR [202–205] and Belle [226]. The leading systematic uncertainties in the untagged $\bar{B} \to \pi\ell\bar{\nu}_\ell$ analyses are associated with modeling the missing momentum reconstruction, with background from $\bar{B} \to X_u\ell\bar{\nu}_\ell$ decays and $e^+e^- \to q\bar{q}$ continuum events, and with varying the form factor used to model $\bar{B} \to \rho\ell\bar{\nu}_\ell$ decays.

Analyses [194, 227] based on reconstructing a B in the $\bar{D}^{(*)}\ell^+\nu_\ell$ decay mode and looking for a $\bar{B} \to \pi\ell\bar{\nu}_\ell$ or $\bar{B} \to \rho\ell\bar{\nu}_\ell$ decay amongst the remaining particles in the event make use of the fact

that the B and $\bar{B}$ are back-to-back in the $\Upsilon(4S)$ frame to construct a discriminant variable that provides a signal-to-noise ratio above unity for all q^2 bins. A related technique was discussed in Ref. [228]. BABAR [227] and Belle [192] have used their samples of B mesons reconstructed in hadronic decay modes to measure exclusive charmless semileptonic decays, resulting in very clean but smaller samples. The dominant systematic uncertainties in the tagged analyses arise from tag calibration.

$|V_{ub}|$ can be obtained from the average $\bar{B} \to \pi\ell\bar{\nu}_\ell$ branching fraction and the measured q^2 spectrum. Fits to the q^2 spectrum using a theoretically motivated parametrization (e.g. "BCL" from Ref. [71]) remove most of the model dependence from theoretical uncertainties in the shape of the spectrum. The most sensitive method for determining $|V_{ub}|$ from $\bar{B} \to \pi\ell\bar{\nu}_\ell$ decays employs a simultaneous fit [6, 206, 217, 218, 229, 230] to measured experimental partial rates and lattice points versus q^2 (or z) to determine $|V_{ub}|$ and the first few coefficients of the expansion of the form factor in z. We quote the result from Ref. [6], which uses as experimental input an average of the measurements in Refs. [192, 202, 205, 226] and an average [231] of the LQCD input from Refs. [206] and [209]. The p-value of the q^2 measurement average is 6%. The average for the total $B^0 \to \pi^-\ell^+\nu_\ell$ branching fraction is obtained by summing up the partial branching fractions:

$$\mathcal{B}(B^0 \to \pi^-\ell^+\nu_\ell) = (1.50 \pm 0.02_{\rm stat} \pm 0.06_{\rm syst}) \times 10^{-4} \tag{76.43}$$

The corresponding value of $|V_{ub}|$ with this approach is found to be

$$|V_{ub}| = (3.70 \pm 0.10 \pm 0.12\,) \times 10^{-3} \quad \text{(exclusive)}, \tag{76.44}$$

where the first uncertainty is experimental and the second is from theory. A consistent result for $|V_{ub}|$ was reported in Ref. [36], which uses the same experimental and lattice-QCD inputs. Adding additional constraints using input from LCSR [222] gives [6] $|V_{ub}| = (3.67 \pm 0.09 \pm 0.12\,) \times 10^{-3}$ (exclusive, LQCD+LCSR). Other recent LCSR estimates [225, 232] have been used to obtain consistent results for $|V_{ub}|$, albeit with slightly higher central values. Ref. [232] also presents results for $|V_{ub}|$ from joint fits that exclude some of the experimental data in order to bring the exclusive values into agreement with the inclusive ones.

76.3.7 $\bar{B}_s \to K\ell\bar{\nu}_\ell$

The LHCb experiment have conducted the first observation of the decay $B_s^0 \to K^-\mu^+\nu_\mu$ and the measurements of its branching fraction normalised to the $B_s^0 \to D_s^-\mu^+\nu_\mu$ decays [233]. The measurement has been performed in two bins of q^2, derived using the B_s^0 flight direction and the known B_s^0 mass. The analysis uses a BDT classifier to suppress semileptonic b-hadron background. The results of the partial branching fractions have been translated into measurements of $|V_{ub}|/|V_{cb}|$ using form factor calculations from LCSR for $q^2 < 7$ GeV^2 [234], and a recent LQCD calculation for $q^2 > 7$ GeV^2 [207]. The results are

$$|V_{ub}|/|V_{cb}| = 0.0607 \pm 0.0021 \pm 0.0030, \;\; q^2 < 7 \text{ GeV}^2, \tag{76.45}$$

$$|V_{ub}|/|V_{cb}| = 0.0946 \pm 0.0041 \pm 0.0068, \;\; q^2 > 7 \text{ GeV}^2, \tag{76.46}$$

where the first uncertainties include also experimental and external input sources, and the latter are due to the form factor calculations. The sizeable discrepancy between the values of $|V_{ub}|/|V_{cb}|$ for the low and high q^2, requires further theoretical and experimental investigation. On the theory side, FLAG [36] perform a joint z-fit to the lattice QCD results in Refs. [207–209], with error inflation to account for the tensions between lattice results for f_0. They then use the form factors for $\bar{B}_s \to K\ell\bar{\nu}_\ell$ and $\bar{B}_s \to D_s^*\ell\bar{\nu}_\ell$ to determine the ratio $|V_{ub}|/|V_{cb}|$ in combination with the LHCb

measurements in the high- and low-q^2 regions, finding good agreement between the two:

$$|V_{ub}|/|V_{cb}| = 0.0819 \pm 0.0029 \pm 0.0072, \ q^2 < 7 \text{ GeV}^2, \tag{76.47}$$
$$|V_{ub}|/|V_{cb}| = 0.0860 \pm 0.0038 \pm 0.0037, \ q^2 > 7 \text{ GeV}^2. \tag{76.48}$$

While the experimental measurement has higher purity in the low q^2 region, the lattice QCD form factors are constrained more reliably in high-q^2 region. RBC/UKQCD recently presented in Ref. [210] an update of their previous calculation. They studied the effect of different strategies for obtaining the form factors $f_{+,0}$ in the continuum limit, finding sizeable differences for f_0, but not f_+. This issue needs to be studied further. In particular, such differences were not seen in a similar study, albeit for D-meson decay form factors [235]. However, the resulting effect on $|V_{ub}|/|V_{cb}|$ is relatively small, as the f_0 form factor enters the determination only via the kinematic constraint at $q^2 = 0$. A very recent analysis in Ref. [236] combines the lattice QCD form factors from Refs. [208, 210] with the LHCb data in $|V_{ub}|/|V_{cb}|$ determinations that are compatible with Eq. (76.48). When they combine their updated LCSR results with the low-q^2 LHCb data, they find $|V_{ub}|/|V_{cb}| = 0.057 \pm 0.005$, compatible with Eq. (76.45), and hence also in tension with Eq. (76.48). Experimental measurements of the differential rates in smaller bins would provide valuable shape constraints and additional compatibility tests, improving the reliability of the $|V_{ub}|/|V_{cb}|$ determinations by reducing the need for extrapolations of form factors.

76.4 Semileptonic b-baryon decays

Summary: A significant sample of Λ_b^0 baryons is available at the LHCb experiment, and methods have been developed to study their semileptonic decays. Both $\Lambda_b^0 \to p\mu\bar{\nu}$ and $\Lambda_b^0 \to \Lambda_c^+\mu\bar{\nu}$ decays have been measured at LHCb, and the ratio of branching fractions to these two decay modes is used to determine the ratio $|V_{ub}/V_{cb}|$.

76.4.1 $\Lambda_b^0 \to \Lambda_c^+\mu\bar{\nu}$ and $\Lambda_b^0 \to p\mu\bar{\nu}$

The $\Lambda_b^0 \to \Lambda_c^+$ and $\Lambda_b^0 \to p$ semileptonic transitions are described in terms of six form factors each. The three form factors corresponding to the vector current can be defined as [237]

$$\begin{aligned}\langle F(p',s')|\bar{q}\,\gamma_\mu\, b|\Lambda_b^0(p,s)\rangle = \bar{u}_F(p',s')\Big\{ & f_0(q^2)\,(M_{\Lambda_b^0} - m_F)\,\frac{q_\mu}{q^2} \\ & + f_+(q^2)\,\frac{M_{\Lambda_b^0} + m_F}{s_+}\left(p_\mu + p'_\mu - \frac{q_\mu}{q^2}\,(M_{\Lambda_b^0}^2 - m_F^2)\right) \\ & + f_\perp(q^2)\left(\gamma_\mu - \frac{2m_F}{s_+}\,p_\mu - \frac{2M_{\Lambda_b^0}}{s_+}\,p'_\mu\right)\Big\}\, u_{\Lambda_b^0}(p,s)\,,\end{aligned} \tag{76.49}$$

where $F = p$ or Λ_c^+ and where we define $s_\pm = (M_{\Lambda_b^0} \pm m_F)^2 - q^2$. At vanishing momentum transfer, $q^2 \to 0$, the kinematic constraint $f_0(0) = f_+(0)$ holds. The form factors are defined in such a way that they correspond to time-like (scalar), longitudinal and transverse polarization with respect to the momentum-transfer q^μ for f_0, f_+ and $f_\perp$, respectively. Likewise, the expression for the

axial-vector current is

$$\begin{aligned}\langle F(p',s')|\bar{q}\,\gamma_\mu\gamma_5\,b|\Lambda_b^0(p,s)\rangle = \\ -\,\bar{u}_F(p',s')\gamma_5\left\{g_0(q^2)\,(M_{\Lambda_b^0}+m_F)\,\frac{q_\mu}{q^2}\right. \\ +g_+(q^2)\,\frac{M_{\Lambda_b^0}-m_F}{s_-}\left(p_\mu+p'_\mu-\frac{q_\mu}{q^2}\,(M^2_{\Lambda_b^0}-m_F^2)\right) \\ \left.+g_\perp(q^2)\left(\gamma_\mu+\frac{2m_F}{s_-}\,p_\mu-\frac{2M_{\Lambda_b^0}}{s_-}\,p'_\mu\right)\right\}u_{\Lambda_b^0}(p,s)\,,\end{aligned} \tag{76.50}$$

with the kinematic constraint $g_0(0) = g_+(0)$ at $q^2 \to 0$.

In the heavy-quark limit, where both the b and c quarks are treated as heavy, all the form factors reduce to the Isgur Wise function ξ_B for baryons [237]:

$$f_0 = f_+ = f_\perp = g_0 = g_+ = g_\perp = \xi_B \tag{76.51}$$

With a light baryon in the final state, the form factors are related through the heavy quark symmetries of the Λ_b^0, reducing the the number of independent form factors to two. It should be noted that the differential $\Lambda_b^0 \to (p/\Lambda_c^+)\mu\bar{\nu}$ decay rates peak at high q^2, so that the kinematic regions where both lattice QCD calculations and experimental measurements are precise are well matched.

The form factors for Λ_b^0 decays have been studied with lattice QCD [238]. Based on these results the differential rates for both $\Lambda_b^0 \to \Lambda_c^+\mu\bar{\nu}$ as well as for $\Lambda_b^0 \to p\mu\bar{\nu}$ can be predicted in the full phase space. In particular, for the experimentally interesting region they find the ratio of decay rates to be [238]

$$\frac{\mathcal{B}(\Lambda_b^0 \to p\mu\bar{\nu})_{q^2>15\,\mathrm{GeV}^2}}{\mathcal{B}(\Lambda_b^0 \to \Lambda_c^+\mu\bar{\nu})_{q^2>7\,\mathrm{GeV}^2}} = (1.471 \pm 0.095 \pm 0.109)\left|\frac{V_{ub}}{V_{cb}}\right|^2 \tag{76.52}$$

where the first uncertainty is statistical and the second, systematic.

76.4.2 *Measurements at LHCb*

The LHCb experiment has measured the branching fractions of the semileptonic decays $\Lambda_b^0 \to \Lambda_c^+\mu\bar{\nu}$ and $\Lambda_b^0 \to p\mu\bar{\nu}$, from which they determine $|V_{ub}|/|V_{cb}|$. This is the first such determination at a hadron collider, the first to use a b baryon decay, and the first observation of $\Lambda_b^0 \to p\mu\bar{\nu}$. Excellent vertex resolution allows the $p\mu$ and production vertices to be separated, which permits the calculation of the transverse momentum $p_\perp$ of the $p\mu$ pair relative to the Λ_b^0 flight direction. The corrected mass, $m_{\mathrm{corr}} = \sqrt{p_\perp^2 + m_{p\mu}^2} + p_\perp$, peaks at the Λ_b^0 mass for signal decays and provides good discrimination against background combinations. The topologically similar decay $\Lambda_b^0 \to \Lambda_c^+\mu\bar{\nu}$ is also measured, which eliminates the need to know the production cross-section or absolute efficiencies. Using vertex and Λ_b^0 mass constraints, q^2 can be determined up to a two-fold ambiguity. The LHCb analysis requires both solutions to be in the high q^2 region to minimise contamination from the low q^2 region. Their result [239], rescaled [6] to take into account the recent branching fraction measurement [240] $\mathcal{B}(\Lambda_c^+ \to pK^-\pi^+) = (6.28 \pm 0.32)\%$, is

$$\frac{\mathcal{B}(\Lambda_b^0 \to p\mu\bar{\nu})_{q^2>15\mathrm{GeV}^2}}{\mathcal{B}(\Lambda_b^0 \to \Lambda_c^+\mu\bar{\nu})_{q^2>7\mathrm{GeV}^2}} = (0.92 \pm 0.04 \pm 0.07) \times 10^{-2} \quad . \tag{76.53}$$

The largest systematic uncertainty is from the measured $\mathcal{B}(\Lambda_c^+ \to pK^-\pi^+)$; uncertainties due to trigger, tracking and the Λ_c^+ selection efficiency are each about 3%.

A LHCb analysis [241] measures the normalized q^2 spectrum and finds good agreement with the shape calculated with lattice QCD [238].

The decay rate for $\Lambda_b^0 \to p\mu\bar{\nu}$ peaks at high q^2 where the calculation of the associated form factors using lattice QCD is under good control. Using the measured ratio from Eq. (76.53) along with the calculated ratio from Ref. [238] (see Eq. (76.52)) results in [6]

$$|V_{ub}|/|V_{cb}| = 0.079 \pm 0.004 \pm 0.004(\Lambda_b). \tag{76.54}$$

where the first uncertainty is experimental and the second is from the LQCD calculation.

76.5 The ratio $|V_{ub}|/|V_{cb}|$

The ratio of matrix elements, $|V_{ub}|/|V_{cb}|$, is often required when testing the compatibility of a set of measurements with theoretical predictions. It can be determined from the ratio of branching fractions and has been directly measured by the LHCb (quoted in the previous sections) and Belle experiments. It can also be calculated based on the $|V_{ub}|$ and $|V_{cb}|$ values quoted earlier in this review.

The average of the LHCb results extracted at high q^2 from B_s and Λ_b decays, taken to be uncorrelated, is

$$|V_{ub}|/|V_{cb}| = 0.083 \pm 0.004 \quad (\Lambda_b,\ B_s). \tag{76.55}$$

The first direct extraction of this ratio from inclusive B decays was recently performed by Belle [176]. Belle measures the ratio of $\bar{B} \to X_u \ell \bar{\nu}_\ell$ and $\bar{B} \to X_c \ell \bar{\nu}_\ell$ branching fractions with a lepton energy threshold of 1.0 GeV. The partial decay widths, omitting the CKM factors, are taken from BLNP and GGOU for $|V_{ub}|$ and the kinetic scheme for $|V_{cb}|$ to extract the ratio of CKM factors. The results are found to be

$$|V_{ub}|/|V_{cb}| = 0.097 \pm 0.008 \quad \text{(BLNP)}, \tag{76.56}$$
$$|V_{ub}|/|V_{cb}| = 0.100 \pm 0.006 \quad \text{(GGOU)}. \tag{76.57}$$

These values are in excellent agreement with $|V_{ub}|/|V_{cb}|$ from independent inclusive determinations, given below, but involve non-zero correlations in both the theoretical and experimental uncertainties. We will therefore leave it out of the combination for this edition.

Given the similarities in the theoretical frameworks used for charmed and charmless decays, we choose to also quote separate ratios of $|V_{ub}|/|V_{cb}|$ for inclusive and exclusive B decays, as discussed earlier:

$$|V_{ub}|/|V_{cb}| = 0.098 \pm 0.006 \quad \text{(inclusive)}, \tag{76.58}$$
$$|V_{ub}|/|V_{cb}| = 0.093 \pm 0.004 \quad \text{(exclusive)}. \tag{76.59}$$

The respective determinations of $|V_{ub}|$ and $|V_{cb}|$ are taken to be uncorrelated in the ratio, although there could be some small cancellations of the uncertainties in both the experimental and the theoretical input. We average the B decay values, along with the B_s and baryonic result in Eq. (76.55), weighting by relative errors to find

$$|V_{ub}|/|V_{cb}| = 0.089 \pm 0.005 \quad \text{(average)}. \tag{76.60}$$

where the uncertainty has been scaled by a factor $\sqrt{\chi^2/2} = 1.6$.

76.6 Lepton flavour universality violation

76.6.1 *Semitauonic decays*

Summary: Semileptonic decays to third-generation leptons provide sensitivity to non-Standard Model amplitudes, such as from a charged Higgs boson [242–245] and from leptoquarks [246–252]. The ratios of branching fractions of semileptonic decays involving tau leptons to those involving $\ell = e/\mu$, $R(D^{(*)}) \equiv \mathcal{B}(\bar{B} \to D^{(*)}\tau\bar{\nu}_\tau)/\mathcal{B}(\bar{B} \to D^{(*)}\ell\bar{\nu}_\ell)$, are predicted with good precision and consistency in the Standard Model [7–11, 27, 28, 30, 47, 48], using a variety of different strategies. Because this ratio is independent of $|V_{cb}|$, it can, in principle, be computed entirely from within the Standard Model, without using experimental decay rate data. For example, in Refs. [7, 9] the lattice-QCD only ratios are obtained as:

$$\begin{aligned} R(D)^{\text{LQCD,FNAL–MILC}} &= 0.284 \pm 0.014 \ , \\ R(D^*)^{\text{LQCD,FNAL–MILC}} &= 0.265 \pm 0.013 \ . \end{aligned} \tag{76.61}$$

Without constraints from experimental data at large recoil, such SM-theory only evaluations tend to be less precise than those obtained from joint fits that employ experimental data as well as Standard-Model theory inputs (lattice-QCD form factors, HQET constraints, etc.). Other recent lattice-QCD only results are found in Refs. [10,11]. Here we use an average of Refs. [27,28,47,48,253] for $R(D)$ and Refs. [27, 28, 30, 63, 253] for $R(D^*)$.

$$\begin{aligned} R(D)^{\text{SM+Exp}} &= 0.298 \pm 0.004 \ , \\ R(D^*)^{\text{LQCD+Exp}} &= 0.254 \pm 0.005 \ . \end{aligned} \tag{76.62}$$

These use various combinations of experimental data, lattice-QCD form factor inputs, HQET constraints, and LCSR estimates and are consistent with the values quoted above.

Measurements [254–261], of these ratios yield higher values; averaging B-tagged measurements of $R(D)$ and $R(D^*)$ at the $\Upsilon(4S)$ and at LHCb yields [6]

$$\begin{aligned} R(D)^{\text{meas}} &= 0.357 \pm 0.029 \ , \\ R(D^*)^{\text{meas}} &= 0.284 \pm 0.012 \ , \end{aligned} \tag{76.63}$$

with a linear correlation of -0.37. These values exceed the Standard Model predictions of Eq. (76.62) by 2.0σ and 2.2σ, respectively. A variety of new physics models have been proposed to explain this excess, see eg. Refs. [242–249] as well as reviews in Refs. [262–264].

76.6.2 *Sensitivity of $\bar{B} \to D^{(*)}\tau\bar{\nu}_\tau$ to additional amplitudes*

In addition to the helicity amplitudes present for decays to $e\bar{\nu}_e$ and $\mu\bar{\nu}_\mu$, decays proceeding through $\tau\bar{\nu}_\tau$ include a scalar amplitude H_s. The differential decay rate is given by [265]

$$\frac{d\Gamma}{dq^2} = \frac{G_F^2 \, |V_{cb}|^2 \, |\mathbf{p}^*_{D^{(*)}}| q^2}{96\pi^3 m_B^2} \left(1 - \frac{m_\tau^2}{q^2}\right)^2 \left[(|H_+|^2 + |H_-|^2 + |H_0|^2) \left(1 + \frac{m_\tau^2}{2q^2}\right) + \frac{3m_\tau^2}{2q^2} |H_s|^2 \right] , \tag{76.64}$$

where $|\mathbf{p}^*_{D^{(*)}}|$ is the 3-momentum of the $D^{(*)}$ in the $\bar{B}$ rest frame and the helicity amplitudes H depend on the four-momentum transfer q^2. All four helicity amplitudes contribute to $\bar{B} \to D^*\tau\bar{\nu}_\tau$, while only H_0 and H_s contribute to $\bar{B} \to D\tau\bar{\nu}_\tau$; as a result, new physics contributions can produce larger effects in the latter mode. Semi-leptonic B decays into a τ lepton provide a

stringent test of the two-Higgs doublet model of type II (2HDMII), i.e. where the two Higgs doublets couple separately to up- and down-type quarks. The distinct feature of the 2HDMII is that the contributions of the charged scalars scale as $m_\tau^2/m_{H^+}^2$, since the couplings to the charged Higgs particles are proportional to the mass of the lepton. As a consequence, one may expect visible effects in decays into a τ, but only small effects for decays into e and μ. The present data disfavors the 2HDMII, see below.

76.6.3 *Measurement of $R(D^{(*)})$*

$\bar{B} \to D^{(*)}\tau\bar{\nu}_\tau$ decays have been studied at the $\Upsilon(4S)$ resonance and in pp collisions. At the $\Upsilon(4S)$, the majority of experimental measurements are based on signatures that consist of a D or D^* meson, an electron or muon (denoted here by ℓ) from the decay $\tau \to \ell\nu_\tau\bar{\nu}_\ell$, a fully-reconstructed decay of the second B meson in the event, and multiple missing neutrinos. One analysis reconstructs the τ in a hadronic mode. The analyses that use hadronic B tags separate signal decays from $\bar{B} \to D^{(*)}\ell\bar{\nu}_\ell$ decays using the lepton momentum and the measured missing mass squared; decays with only a single missing neutrino peak sharply at zero in this variable, while the signal is spread out to positive values. When a semileptonic B tag is used, the discrimination between signal and $\bar{B} \to D^{(*)}\ell\bar{\nu}_\ell$ decays comes from the calorimeter energy that is not associated with any particle used in the reconstruction of the B meson candidates, the measured missing mass squared and the cosine of the angle between the $D^*\ell$ system and its parent B meson, which is calculated under the assumption that only one particle (a neutrino) is missing. In both these approaches, background from $\bar{B} \to D^{**}\ell\bar{\nu}_\ell$ decays with one or more unreconstructed particles is challenging to separate from signal, as is background from $\bar{B} \to D^{(*)}H_{\bar{c}}X$ (where $H_{\bar{c}}$ is a hadron containing a $\bar{c}$ quark) decays. The leading sources of systematic uncertainty are due to the limited size of simulation samples used in constructing the PDFs, the composition of the D^{**} states, efficiency corrections, and cross-feed (swapping soft particles between the signal and tag B).

The most precise measurement from Belle [258] uses semileptonic B tags and leptonic τ decays to simultaneously measure $R(D^*)$ and $R(D)$. The measurement combines results from charged and neutral B decays for both $R(D^*)$ and $R(D)$, and is compatible with the Standard Model expectation to approximately 1σ. The first result from Belle II [259] uses a hadronic tag to measure $R(D^*)$ in $\bar{B} \to D^*\tau^-\bar{\nu}_\tau$ decays with a 189 fb^{-1} dataset. The statistical power of the Belle II dataset has been found to outperform that of Belle in this channel.

In addition to the ratio measurements, the Belle experiment has performed polarization measurements of the τ [257] and D^* [266] respectively. The τ polarization measurement uses hadronic B tags and τ^- decays to $\pi^-\nu_\tau$ or $\rho^-\nu_\tau$. The main discriminant variables are the measured missing mass squared and the unassociated calorimeter energy. This measurement provides the first determination of the τ polarization in the $\bar{B} \to D^*\tau\bar{\nu}_\tau$ decay, $\mathcal{P}_\tau(D^*) = -0.38 \pm 0.51\ ^{+0.21}_{-0.16}$, compatible with the Standard Model expectation [30], $\mathcal{P}_\tau(D^*) = -0.476^{+0.037}_{-0.034}$.

The main uncertainties on the $R(D^*)$ measurement come from the composition of the hadronic B background and from modeling of semileptonic B decays and mis-reconstructed D^* mesons. The D^* polarization measurement uses an inclusive tag approach based on Refs. [267, 268], and reconstructs the τ decays in $\ell\nu_\tau\bar{\nu}_\ell$ and $\pi^+\bar{\nu}_\tau$ channels. The main discriminant variables are $X_{\rm miss}$, a quantity that approximates missing mass but does not depend on tag B reconstruction, the visible energy of the event, and the beam-energy constrained mass, $M_{\rm bc}$, of the inclusively reconstructed tag side B. This measurement provides the first determination of the D^* longitudinal polarization fraction in the $\bar{B} \to D^*\tau\bar{\nu}_\tau$ decay, $\mathcal{F}_L(D^*) = -0.38 \pm 0.60\ ^{+0.08}_{-0.04}$, compatible with the Standard Model expectation [269] within 1.7σ.

The LHCb experiment has performed a simultaneous analysis of $R(D^*)$ and $R(D)$ where $\tau \to \mu\nu_\tau\bar{\nu}_\mu$. The reconstructed decay modes are $\bar{B}^0 \to D^{*+}\tau^-\bar{\nu}_\tau$ with $D^{*+} \to D^0\pi^+$, $B^- \to D^{*0}\tau^-\bar{\nu}_\tau$

with $D^{*0} \to D^0\pi^0$ and $D^{*0} \to D^0\pi^0$, and $B^- \to D^0\tau^-\bar{\nu}_\tau$. Their analysis [261] takes advantage of the measurable flight lengths of b and c hadrons and τ leptons. A multivariate discriminant is used to select decays where no additional charged particles are consistent with coming from the signal decay vertices. The separation between the primary and B decay vertices is used to calculate the momentum of the B decay products transverse to the B flight direction. The longitudinal component of the B momentum can be estimated based on the visible decay products; this allows a determination of the B rest frame, with modest resolution, and enables the calculation of similar discrimination variables to those available at the e^+e^- B factories. The (rest frame) muon energy, missing mass-squared and q^2 are used in a 3-d fit.

A complementary LHCb result [260] on $R(D^*)$ uses three-prong τ decays that take advantage of their excellent vertex resolution to isolate the τ decay from hadronic background. A 3-d fit is performed to determine the signal yield, based on the τ-ν_τ pair q^2, the τ lifetime, as well as a boosted decision tree classifier based on isolation, invariant mass and flight distance information. The leading sources of systematic uncertainty are due to the size of the simulation sample used in constructing the fit templates, uncertainties in modelling the background from hadronic $\bar{B} \to D^{(*)}H_{\bar{c}}X$ decays, as well as reconstruction and trigger effects. The result is normalized to $B^0 \to D^{*-}\pi^+\pi^-\pi^+$ and found to be 1σ from the Standard Model expectation (using the expectation value quoted here). An analogous measurement of $B_c \to J/\psi\tau\bar{\nu}_\tau$ was performed by the LHCb measurement [270], in leptonic τ decays. The result, $R(J/\psi) = 0.71 \pm 0.17 \pm 0.18$, while relatively high is compatible to within 2σ of a recent Standard Model evaluation [271] based on a latttice-QCD calculation [272] of the form factors. Systematic uncertainties are dominated by form factors, as B_c decays are relatively unexplored.

Measurements from BABAR [254, 255], Belle [256–258], Belle II [259] and LHCb [260, 261] result in values for $R(D)$ and $R(D^*)$ that exceed Standard Model predictions. Table 76.3 lists these values and their average. The simultaneous measurements of $R(D)$ and $R(D^*)$ have linear correlation coefficients of -0.27 (BABAR [254,255]), -0.49 (Belle hadronic tag [256]), -0.51 (Belle semileptonic tag [258]), and 0.43 (LHCb $\tau^- \to \mu^-\nu_\tau\bar{\nu}_\mu$); the $R(D)$ and $R(D^*)$ averages have a correlation of -0.40. Two early untagged Belle measurements [267, 268] are subject to larger systematic uncertainties, with a breakdown of the respective contributions that is inconsistent with the more recent determinations, hence they cannot be reliably combined in the average. All three experiments assume the Standard Model kinematic distributions for $\bar{B} \to D^{(*)}\tau\bar{\nu}_\tau$ in their determinations of the branching fraction ratios.

Table 76.3: Measurements of $R(D)$ and $R(D^*)$, their correlations, ρ, and the combined averages [6].

		$R(D) \times 10^2$	$R(D^*) \times 10^2$	ρ
BABAR [254, 255]	B^0, B^+	$44.0 \pm 5.8 \pm 4.2$	$33.2 \pm 2.4 \pm 1.8$	-0.27
Belle [256]	B^0, B^+	$37.5 \pm 6.4 \pm 2.6$	$29.3 \pm 3.8 \pm 1.5$	-0.49
Belle [257, 273]	B^0, B^+		$27.0 \pm 3.5\ ^{+\ 2.8}_{-\ 2.5}$	
Belle [258]	B^0, B^+	$30.7 \pm 3.7 \pm 1.6$	$28.3 \pm 1.8 \pm 1.4$	-0.51
LHCb [261]	B^+ ($R(D)$), B^0	$44.1 \pm 6.0 \pm 6.6$	$28.1 \pm 1.8 \pm 2.4$	-0.43
LHCb [260]	B^0		$25.7 \pm 1.2 \pm 1.8$	
Belle II [259]	B^0, B^+		$26.2^{+4.1+3.5}_{-3.9-3.2}$	
Average	B^0, B^+	35.7 ± 2.9	28.4 ± 1.2	-0.40

The measurement combination in the $R(D) - R(D^*)$ plane is shown in Fig. 76.2, compared

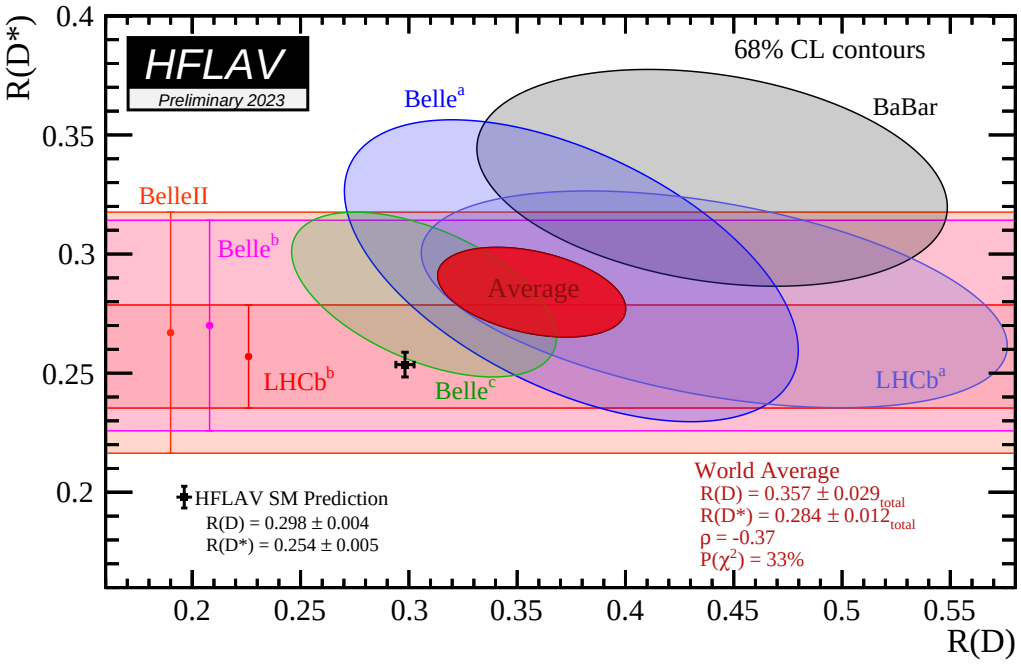

Figure 76.2: Measurements of $R(D)$ and $R(D^*)$ and their two-dimensional average compared with the average predictions for $R(D)$ and $R(D^*)$ given in Eq. 76.62. Contours correspond to 68% CL. The experiment-lattice QCD-HQET predictions and the experimental average deviate from each other by 3.3σ.

with the predictions in Eq. (76.61) (LQCD) and Eq. (76.62) (Experiment+LQCD+HQET). The measurement combination is based on Ref. [6] and online updates with the inclusion of recent results from LHCb and Belle II. The tension between the Standard Model prediction in Eq. (76.62) and the measurements is at the level of 2.0σ ($R(D)$) and 2.2σ ($R(D^*)$); if one considers these deviations together the significance is 3.3σ. This motivates speculation on possible new physics contributions. The measurements reported in Refs. [259, 260, 273] are all in reasonable agreement with the Standard-Model predictions. There is some tension in the combination coming from the BABAR measurement and the most recent LHCb measurement [261]. The BABAR measurement is the only one to claim a deviation from the Standard Model of more than 3σ, although the $p-$value of the full combination is an acceptable 33%.

The current discussion of $R(D)$ and $R(D^*)$ may be embedded in the theoretical analysis of the other anomalies that have been observed in semileptonic FCNC ($b \to s\ell\ell$) transitions. More sophisticated approaches fit the data to a general effective Hamiltonian. Matching this effective Hamiltonian to simplified models, the current situation of the anomalies seems to be compatible with scenarios with an additional Z' or a leptoquark scenario, see eg. [246–252].

76.6.4 *Measurements of* $R(X)$

We note that in addition to exclusive modes, inclusive modes also offer an opportunity to test the presence of non-Standard Model contributions, although typically with lower precision. The first measurement of $R(X)$ from a B-factory was recently performed by Belle II [274], $R(X) = 0.228 \pm 0.039$, and found to be compatible with an average of Standard Model predictions $R(X) = 0.223 \pm 0.005$ [275–277]. Prior measurements of the branching fractions of $b \to X\tau\nu$ were performed

by LEP experiments and also found to be compatible with Standard Model predictions.

76.6.5 *Ratios of semileptonic decay rates with e to μ final states*

Several tests of lepton flavor universality in semileptonic B decays have recently been undertaken at Belle and Belle II. This includes ratios of rates to electron and muon modes (i.e. $R(e/\mu)$) performed as part of CKM matrix element extraction analyses (Table 76.4), as well as dedicated flavour dependent angular analyses [278]. Refs. [62, 64, 65] provide measurements of LFUV in $\bar{B} \to D^* \ell \bar{\nu}$ decays at Belle (untagged, and hadron tagged) and Belle II (hadron tagged). The corresponding theoretical prediction is $\mathcal{B}(B \to D^* e\nu)/\mathcal{B}(B \to D^* \mu\nu) = 1.0041 \pm 0.0001$ [33]. Refs. [176,279] provide measurements of LFUV in $B \to X_c \ell \bar{\nu}$ in hadron tagged events at Belle and Belle II, where the theoretical expectation is $\mathcal{B}(B \to X_c e\nu)/\mathcal{B}(B \to X_c \mu\nu) = 1.006 \pm 0.001$ [276]. Finally, Ref. [173] provides a result for LFUV in $B \to X_u \ell\nu$ decays where the ratio is expected to be close to 1, as in the $B \to X_c \ell\nu$ case. With the exception of the charmless decay measurement, the experimental uncertainties are dominated by lepton identification uncertainties that do not cancel in the ratios. All results are found to be highly compatible with SM expectations.

Table 76.4: Measurements of $R(e/\mu) = \mathcal{B}(B \to Xe\nu)/\mathcal{B}(B \to X\mu\nu)$ where the specific decay process is listed.

Ref.	Decay	$R(e/\mu) \times 100$
Belle [64]	$\bar{B} \to D^* \ell \bar{\nu}$	$99.2 \pm 2.3 \pm 2.3$
Belle [62]	$B^0 \to D^{*+} \ell\nu$	$101 \pm 1 \pm 3$
Belle II [65]	$B^0 \to D^{*+} \ell\nu$	$99.8 \pm 0.9 \pm 2.0$
Belle II [279]	$B \to X_c \ell\nu$	$100.7 \pm 0.9 \pm 1.9$
Belle [176]	$B \to X_c \ell\nu$	$100.3 \pm 0.5 \pm 2.4$
Belle [173]	$B \to X_u \ell\nu$	$97 \pm 9 \pm 4$

76.7 Conclusion

The study of semileptonic B meson decays continues to be an active area for both theory and experiment. The application of HQE calculations to inclusive decays is well established, and fits to moments of $\bar{B} \to X_c \ell \bar{\nu}_\ell$ decays provide precise values for $|V_{cb}|$ and, in conjunction with input on m_c or from $B \to X_s \gamma$ decays, provide precise and consistent values for m_b. Recent developments will make use of more types of moments and better theoretical inputs to constrain higher order effects. Further into the future, new nonperturbative methods to compute inclusive decay rates, for example, in lattice QCD [280–282], may provide interesting new insights.

The determination of $|V_{ub}|$ from inclusive $\bar{B} \to X_u \ell \bar{\nu}_\ell$ decays is based on multiple calculational approaches and independent measurements over a variety of kinematic regions, all of which provide consistent results. Further progress in this area is possible, but will require better theoretical control over higher-order terms, improved experimental knowledge of the $\bar{B} \to X_c \ell \bar{\nu}_\ell$ background and improvements to the modeling of the $\bar{B} \to X_u \ell \bar{\nu}_\ell$ signal distributions.

In both $b \to u$ and $b \to c$ exclusive channels there has been significant recent progress in lattice-QCD calculations, resulting in improved precision on both $|V_{ub}|$ and $|V_{cb}|$. These calculations now provide information on the form factors well away from the high q^2 region, allowing better use of experimental data. For $|V_{cb}|$ recent measurements have provided binned data enabling model-independent fits.

The values from the inclusive and exclusive determinations of $|V_{cb}|$ and $|V_{ub}|$ are only marginally consistent. This is a long-standing puzzle that the recent improvements have, unfortunately, not yet resolved.

Both $|V_{cb}|$ and $|V_{ub}|$ are indispensable inputs into unitarity triangle fits. In particular, knowing $|V_{ub}|$ with good precision allows a test of CKM unitarity in a most direct way, by comparing the length of the $|V_{ub}|$ side of the unitarity triangle with the measurement of $\sin(2\beta)$. This comparison of a "tree" process ($b \to u$) with a "loop-induced" process ($B^0 - \bar{B}^0$ mixing) provides sensitivity to possible contributions from new physics.

The observation of semileptonic decays into τ leptons has opened a new window to the physics of the third generation. The measurements indicate a tension between the data and Standard-Model predictions, which could be a hint for new physics, manifesting itself as a violation of lepton universality beyond the Standard-Model couplings to the Higgs. It should be noted that none of the most recent measurements alone claim discovery of a deviation from the Standard Model. Combining the data of the semitauonic decays with the anomalies observed in the FCNC $b \to s\ell\ell$ transitions allows an interpretation in terms of additional Z' or in terms of additional leptoquarks, but the current data does not allow us to draw a definite conclusion.

Acknowledgements

We thank J. Flynn, E. Kou, C. Schwanda, and K. Vos for useful discussions and comments on this review, and A. Vaquero for creating Fig. 76.1. Previous assistance from D. Ferlewicz, P. Gambino, S. Hashimoto, Z. Ligeti, and M. Rotondo is also acknowledged.

References

[1] See"Leptonic Decays of Charged Pseudoscalar Mesons" by J.L. Rosner, S.L. Stone, and R. Van de Water in this *Review*.

[2] R. L. Workman and Others (Particle Data Group), PTEP **2022**, 083C01 (2022).

[3] See"Heavy-Quark and Soft-Collinear Effective Theory" by C.W. Bauer and M. Neubert in this *Review*.

[4] See "Lattice Quantum Chromodynamics" by S. Hashimoto, J. Laiho, and S.R. Sharpe in this *Review*.

[5] See "Production and Decay of b-Flavored Hadrons" by P. Eerola, M. Kreps and Y. Kwon in this *Review*.

[6] Y. S. Amhis *et al.* (Heavy Flavor Averaging Group, HFLAV), Phys. Rev. D **107**, 5, 052008 (2023), [arXiv:2206.07501].

[7] J. A. Bailey *et al.* (Fermilab Lattice and MILC), Phys. Rev. **D92**, 3, 034506 (2015), [arXiv:1503.07237].

[8] H. Na *et al.* (HPQCD), Phys. Rev. **D92**, 5, 054510 (2015), [Erratum: Phys. Rev.D93,no.11,119906(2016)], [arXiv:1505.03925].

[9] A. Bazavov *et al.* (Fermilab Lattice, MILC), Eur. Phys. J. C **82**, 12, 1141 (2022), [Erratum: Eur.Phys.J.C 83, 21 (2023)], [arXiv:2105.14019].

[10] J. Harrison and C. T. H. Davies (2023), [arXiv:2304.03137].

[11] Y. Aoki *et al.* (JLQCD) (2023), [arXiv:2306.05657].

[12] J. Harrison and C. T. H. Davies (HPQCD), Phys. Rev. D **105**, 9, 094506 (2022), [arXiv:2105.11433].

[13] N. Isgur and M. B. Wise, Phys. Lett. **B232**, 113 (1989); N. Isgur and M. B. Wise, Phys. Lett. **B237**, 527 (1990).

[14] M. A. Shifman and M. B. Voloshin, Sov. J. Nucl. Phys. **47**, 511 (1988), [Yad. Fiz.47,801(1988)].

[15] A. V. Manohar and M. B. Wise, Camb. Monogr. Part. Phys. Nucl. Phys. Cosmol. **10**, 1 (2000).

[16] H. Georgi, Phys. Lett. **B240**, 447 (1990).

[17] A. F. Falk *et al.*, Nucl. Phys. **B343**, 1 (1990).

[18] E. Eichten and B. R. Hill, Phys. Lett. **B234**, 511 (1990).

[19] A. Sirlin, Nucl. Phys. **B196**, 83 (1982).

[20] J. A. Bailey *et al.* (Fermilab Lattice, MILC), Phys. Rev. D **89**, 11, 114504 (2014), [arXiv:1403.0635].

[21] C. G. Boyd, B. Grinstein and R. F. Lebed, Phys. Rev. Lett. **74**, 4603 (1995), [hep-ph/9412324].

[22] C. G. Boyd, B. Grinstein and R. F. Lebed, Phys. Lett. B **353**, 306 (1995), [hep-ph/9504235].

[23] C. G. Boyd, B. Grinstein and R. F. Lebed, Nucl. Phys. B **461**, 493 (1996), [hep-ph/9508211].

[24] C. G. Boyd, B. Grinstein and R. F. Lebed, Phys. Rev. D **56**, 6895 (1997), [hep-ph/9705252].

[25] B. Grinstein and A. Kobach, Phys. Lett. **B771**, 359 (2017), [arXiv:1703.08170].

[26] I. Caprini, L. Lellouch and M. Neubert, Nucl. Phys. **B530**, 153 (1998), [hep-ph/9712417].

[27] M. Bordone, M. Jung and D. van Dyk (2019), [arXiv:1908.09398].

[28] F. U. Bernlochner *et al.*, Phys. Rev. **D95**, 11, 115008 (2017), [erratum: Phys. Rev.D97,no.5,059902(2018)], [arXiv:1703.05330].

[29] D. Bigi, P. Gambino and S. Schacht, Phys. Lett. **B769**, 441 (2017), [arXiv:1703.06124].

[30] P. Gambino, M. Jung and S. Schacht, Phys. Lett. **B795**, 386 (2019), [arXiv:1905.08209].

[31] F. U. Bernlochner, Z. Ligeti and D. J. Robinson, Phys. Rev. **D100**, 1, 013005 (2019), [arXiv:1902.09553].

[32] F. U. Bernlochner *et al.*, Phys. Rev. **D96**, 9, 091503 (2017), [arXiv:1708.07134].

[33] F. U. Bernlochner *et al.*, Phys. Rev. D **106**, 9, 096015 (2022), [arXiv:2206.11281].

[34] M. Jung, private communication.

[35] J. Harrison, C. Davies and M. Wingate (HPQCD), Phys. Rev. **D97**, 5, 054502 (2018), [arXiv:1711.11013].

[36] Y. Aoki *et al.* (Flavour Lattice Averaging Group (FLAG)), Eur. Phys. J. C **82**, 10, 869 (2022), [arXiv:2111.09849].

[37] I. I. Y. Bigi *et al.*, Phys. Rev. **D52**, 196 (1995), [hep-ph/9405410].

[38] A. Kapustin *et al.*, Phys. Lett. **B375**, 327 (1996), [hep-ph/9602262].

[39] P. Gambino, T. Mannel and N. Uraltsev, Phys. Rev. **D81**, 113002 (2010), [arXiv:1004.2859].

[40] M. A. Shifman, N. G. Uraltsev and A. I. Vainshtein, Phys. Rev. D **51**, 2217 (1995), [Erratum: Phys.Rev.D 52, 3149 (1995)], [hep-ph/9405207].

[41] A. Czarnecki, K. Melnikov and N. Uraltsev, Phys. Rev. D **57**, 1769 (1998), [hep-ph/9706311].

[42] P. Gambino, T. Mannel and N. Uraltsev, JHEP **10**, 169 (2012), [arXiv:1206.2296].

[43] N. Gubernari, A. Kokulu and D. van Dyk, JHEP **01**, 150 (2019), [arXiv:1811.00983].

[44] L. Lellouch, Nucl. Phys. B **479**, 353 (1996), [hep-ph/9509358].

[45] M. Di Carlo *et al.*, Phys. Rev. D **104**, 5, 054502 (2021), [arXiv:2105.02497].

[46] G. Martinelli, S. Simula and L. Vittorio (2021), [arXiv:2105.07851].

[47] D. Bigi and P. Gambino, Phys. Rev. **D94**, 9, 094008 (2016), [arXiv:1606.08030].

[48] G. Martinelli, S. Simula and L. Vittorio, Phys. Rev. D **105**, 3, 034503 (2022), [arXiv:2105.08674].

[49] G. Martinelli, S. Simula and L. Vittorio, Eur. Phys. J. C **82**, 12, 1083 (2022), [arXiv:2109.15248].

[50] G. Martinelli, S. Simula and L. Vittorio, JHEP **08**, 022 (2022), [arXiv:2202.10285].

[51] G. Martinelli *et al.*, Phys. Rev. D **106**, 9, 093002 (2022), [arXiv:2204.05925].

[52] J. M. Flynn, A. Jüttner and J. T. Tsang (2023), [arXiv:2303.11285].

[53] D. Buskulic *et al.* (ALEPH), Phys. Lett. **B395**, 373 (1997).

[54] G. Abbiendi *et al.* (OPAL), Phys. Lett. **B482**, 15 (2000), [hep-ex/0003013].

[55] P. Abreu *et al.* (DELPHI), Phys. Lett. **B510**, 55 (2001), [hep-ex/0104026].

[56] J. Abdallah *et al.* (DELPHI), Eur. Phys. J. **C33**, 213 (2004), [hep-ex/0401023].

[57] N. E. Adam *et al.* (CLEO), Phys. Rev. **D67**, 032001 (2003), [hep-ex/0210040].

[58] B. Aubert *et al.* (BaBar), Phys. Rev. **D77**, 032002 (2008), [arXiv:0705.4008].

[59] B. Aubert *et al.* (BaBar), Phys. Rev. Lett. **100**, 231803 (2008), [arXiv:0712.3493].

[60] B. Aubert *et al.* (BaBar), Phys. Rev. **D79**, 012002 (2009), [arXiv:0809.0828].

[61] W. Dungel *et al.* (Belle), Phys. Rev. **D82**, 112007 (2010), [arXiv:1010.5620].

[62] E. Waheed *et al.* (Belle), Phys. Rev. D **100**, 5, 052007 (2019), [Erratum: Phys.Rev.D 103, 079901 (2021)], [arXiv:1809.03290].

[63] J. P. Lees *et al.* (BaBar), Phys. Rev. Lett. **123**, 9, 091801 (2019), [arXiv:1903.10002].

[64] M. T. Prim *et al.* (Belle), Phys. Rev. D **108**, 1, 012002 (2023), [arXiv:2301.07529].

[65] I. Adachi *et al.* (Belle-II), Phys. Rev. D **108**, 9, 092013 (2023), [arXiv:2310.01170].

[66] D. Ferlewicz, P. Urquijo and E. Waheed, Phys. Rev. D **103**, 7, 073005 (2021), [arXiv:2008.09341].

[67] D. Bigi, P. Gambino and S. Schacht, JHEP **11**, 061 (2017), [arXiv:1707.09509].

[68] B. Aubert *et al.* (BaBar), Phys. Rev. Lett. **104**, 011802 (2010), [arXiv:0904.4063].

[69] R. Glattauer *et al.* (Belle), Phys. Rev. **D93**, 3, 032006 (2016), [arXiv:1510.03657].

[70] S. Aoki *et al.* (Flavour Lattice Averaging Group) (2019), [arXiv:1902.08191].

[71] C. Bourrely, I. Caprini and L. Lellouch, Phys. Rev. **D79**, 013008 (2009), [Erratum: Phys. Rev.D82,099902(2010)], [arXiv:0807.2722].

[72] C. J. Monahan *et al.*, Phys. Rev. D **95**, 11, 114506 (2017), [arXiv:1703.09728].

[73] E. McLean *et al.*, Phys. Rev. D **101**, 7, 074513 (2020), [arXiv:1906.00701].

[74] E. McLean *et al.*, Phys. Rev. D **99**, 11, 114512 (2019), [arXiv:1904.02046].

[75] R. Aaij *et al.* (LHCb), Phys. Rev. D **101**, 7, 072004 (2020), [arXiv:2001.03225].

[76] R. Aaij *et al.* (LHCb), Phys. Rev. D **104**, 3, 032005 (2021), [arXiv:2103.06810].

[77] R. Aaij *et al.* (LHCb), JHEP **12**, 144 (2020), [arXiv:2003.08453].

[78] A. V. Manohar and M. B. Wise, Phys. Rev. **D49**, 1310 (1994), [hep-ph/9308246].

[79] I. I. Y. Bigi *et al.*, Phys. Rev. Lett. **71**, 496 (1993), [,201(1993)], [hep-ph/9304225]; I. I. Y. Bigi *et al.*, Phys. Lett. **B323**, 408 (1994), [hep-ph/9311339].

[80] D. Benson *et al.*, Nucl. Phys. **B665**, 367 (2003), [hep-ph/0302262].

[81] M. Gremm and A. Kapustin, Phys. Rev. **D55**, 6924 (1997), [hep-ph/9603448].

[82] B. M. Dassinger, T. Mannel and S. Turczyk, JHEP **03**, 087 (2007), [hep-ph/0611168].

[83] I. I. Bigi, N. Uraltsev and R. Zwicky, Eur. Phys. J. **C50**, 539 (2007), [hep-ph/0511158].

[84] T. Mannel, S. Turczyk and N. Uraltsev, JHEP **11**, 109 (2010), [arXiv:1009.4622].

[85] A. Pak and A. Czarnecki, Phys. Rev. **D78**, 114015 (2008), [arXiv:0808.3509].

[86] S. Biswas and K. Melnikov, JHEP **02**, 089 (2010), [arXiv:0911.4142].

[87] P. Gambino, JHEP **09**, 055 (2011), [arXiv:1107.3100].

[88] M. Fael, K. Schönwald and M. Steinhauser, Phys. Rev. D **104**, 1, 016003 (2021), [arXiv:2011.13654].

[89] P. Gambino and N. Uraltsev, Eur. Phys. J. **C34**, 181 (2004), [hep-ph/0401063].

[90] V. Aquila *et al.*, Nucl. Phys. **B719**, 77 (2005), [hep-ph/0503083].

[91] M. E. Luke, M. J. Savage and M. B. Wise, Phys. Lett. B **343**, 329 (1995), [hep-ph/9409287].

[92] M. E. Luke, M. J. Savage and M. B. Wise, Phys. Lett. B **345**, 301 (1995), [hep-ph/9410387].

[93] T. Becher, H. Boos and E. Lunghi, JHEP **12**, 062 (2007), [arXiv:0708.0855].

[94] A. Alberti *et al.*, Nucl. Phys. **B870**, 16 (2013), [arXiv:1212.5082].

[95] A. Alberti, P. Gambino and S. Nandi, JHEP **01**, 147 (2014), [arXiv:1311.7381].

[96] T. Mannel, A. A. Pivovarov and D. Rosenthal, Phys. Rev. **D92**, 5, 054025 (2015), [arXiv:1506.08167].

[97] T. Mannel and A. A. Pivovarov, Phys. Rev. D **100**, 9, 093001 (2019), [arXiv:1907.09187].

[98] T. Mannel, D. Moreno and A. A. Pivovarov, Phys. Rev. D **105**, 5, 054033 (2022), [arXiv:2112.03875].

[99] C. Breidenbach *et al.*, Phys. Rev. **D78**, 014022 (2008), [arXiv:0805.0971].

[100] I. Bigi *et al.*, JHEP **04**, 073 (2010), [arXiv:0911.3322].

[101] A. Kobach and S. Pal, Phys. Lett. **B772**, 225 (2017), [arXiv:1704.00008].

[102] J. Heinonen and T. Mannel, Nucl. Phys. **B889**, 46 (2014), [arXiv:1407.4384].

[103] P. Gambino, K. J. Healey and S. Turczyk, Phys. Lett. **B763**, 60 (2016), [arXiv:1606.06174].

[104] T. Mannel and K. K. Vos, JHEP **06**, 115 (2018), [arXiv:1802.09409].

[105] M. Fael, T. Mannel and K. Keri Vos, JHEP **02**, 177 (2019), [arXiv:1812.07472].

[106] I. I. Y. Bigi *et al.*, Phys. Rev. **D50**, 2234 (1994), [hep-ph/9402360].

[107] A. H. Hoang, Z. Ligeti and A. V. Manohar, Phys. Rev. Lett. **82**, 277 (1999), [hep-ph/9809423].

[108] A. H. Hoang, Z. Ligeti and A. V. Manohar, Phys. Rev. **D59**, 074017 (1999), [hep-ph/9811239].

[109] A. H. Hoang and T. Teubner, Phys. Rev. **D60**, 114027 (1999), [hep-ph/9904468].

[110] A. Hoang, P. Ruiz-Femenia and M. Stahlhofen, JHEP **10**, 188 (2012), [arXiv:1209.0450].

[111] M. Fael, K. Schönwald and M. Steinhauser, Phys. Rev. Lett. **125**, 5, 052003 (2020), [arXiv:2005.06487].

[112] S. E. Csorna *et al.* (CLEO), Phys. Rev. **D70**, 032002 (2004), [hep-ex/0403052].

[113] A. H. Mahmood *et al.* (CLEO), Phys. Rev. **D70**, 032003 (2004), [hep-ex/0403053].

[114] B. Aubert *et al.* (BaBar), Phys. Rev. **D69**, 111103 (2004), [hep-ex/0403031].

[115] B. Aubert *et al.* (BaBar), Phys. Rev. **D69**, 111104 (2004), [hep-ex/0403030].

[116] C. Schwanda *et al.* (Belle), Phys. Rev. **D75**, 032005 (2007), [hep-ex/0611044].

[117] P. Urquijo *et al.* (Belle), Phys. Rev. **D75**, 032001 (2007), [hep-ex/0610012].

[118] J. Abdallah *et al.* (DELPHI), Eur. Phys. J. **C45**, 35 (2006), [hep-ex/0510024].

[119] D. Acosta *et al.* (CDF), Phys. Rev. **D71**, 051103 (2005), [hep-ex/0502003].

[120] B. Aubert *et al.* (BaBar), Phys. Rev. **D81**, 032003 (2010), [arXiv:0908.0415].

[121] R. van Tonder *et al.* (Belle), Phys. Rev. D **104**, 11, 112011 (2021), [arXiv:2109.01685].

[122] F. Abudinén *et al.* (Belle-II), Phys. Rev. D **107**, 7, 072002 (2023), [arXiv:2205.06372].

[123] A. Limosani *et al.* (Belle), Phys. Rev. Lett. **103**, 241801 (2009), [arXiv:0907.1384].

[124] C. Schwanda *et al.* (Belle), Phys. Rev. **D78**, 032016 (2008), [arXiv:0803.2158].

[125] B. Aubert *et al.* (BaBar), Phys. Rev. **D72**, 052004 (2005), [hep-ex/0508004].

[126] B. Aubert *et al.* (BaBar), Phys. Rev. Lett. **97**, 171803 (2006), [hep-ex/0607071].

[127] S. Chen *et al.* (CLEO), Phys. Rev. Lett. **87**, 251807 (2001), [hep-ex/0108032].

[128] M. Battaglia *et al.*, eConf **C0304052**, WG102 (2003), [Phys. Lett.B556,41(2003)], [hep-ph/0210319].

[129] B. Aubert *et al.* (BaBar), Phys. Rev. Lett. **93**, 011803 (2004), [hep-ex/0404017].

[130] O. Buchmüller and H. Flächer, `hep-ph/0507253` updated in Ref. [283].

[131] C. W. Bauer *et al.*, Phys. Rev. **D70**, 094017 (2004), updated in Ref. [283], [hep-ph/0408002].

[132] P. Gambino and C. Schwanda, Phys. Rev. **D89**, 1, 014022 (2014), [arXiv:1307.4551].

[133] A. Alberti *et al.*, Phys. Rev. Lett. **114**, 6, 061802 (2015), [arXiv:1411.6560].

[134] M. Bordone, B. Capdevila and P. Gambino, Phys. Lett. B **822**, 136679 (2021), [arXiv:2107.00604].

[135] M. Antonelli *et al.*, Phys. Rept. **494**, 197 (2010), see section 5.4.2, [arXiv:0907.5386].

[136] See"Quark Masses" by A.V. Manohar, L.P. Lellouch , and R.M. Barnett in this *Review*.

[137] M. Fael, K. Schönwald and M. Steinhauser, Phys. Rev. D **103**, 1, 014005 (2021), [arXiv:2011.11655].

[138] F. Bernlochner *et al.*, JHEP **10**, 068 (2022), [arXiv:2205.10274].

[139] N. Uraltsev, Int. J. Mod. Phys. **A14**, 4641 (1999), [hep-ph/9905520].

[140] M. Neubert, Phys. Rev. **D49**, 4623 (1994), [hep-ph/9312311]; M. Neubert, Phys. Rev. **D49**, 3392 (1994), [hep-ph/9311325].

[141] I. I. Y. Bigi *et al.*, Int. J. Mod. Phys. **A9**, 2467 (1994), [hep-ph/9312359].

[142] C. W. Bauer, M. E. Luke and T. Mannel, Phys. Rev. **D68**, 094001 (2003), [hep-ph/0102089].

[143] M. Benzke *et al.*, Phys. Rev. Lett. **106**, 141801 (2011), [arXiv:1012.3167].

[144] A. Gunawardana and G. Paz, JHEP **11**, 141 (2019), [arXiv:1908.02812].

[145] F. U. Bernlochner *et al.* (SIMBA), Phys. Rev. Lett. **127**, 10, 102001 (2021), [arXiv:2007.04320].

[146] M. Neubert, Phys. Lett. **B513**, 88 (2001), [hep-ph/0104280].

[147] M. Neubert, Phys. Lett. **B543**, 269 (2002), [hep-ph/0207002].

[148] A. K. Leibovich, I. Low and I. Z. Rothstein, Phys. Rev. **D61**, 053006 (2000), [hep-ph/9909404].

[149] A. K. Leibovich, I. Low and I. Z. Rothstein, Phys. Rev. **D62**, 014010 (2000), [hep-ph/0001028].

[150] A. K. Leibovich, I. Low and I. Z. Rothstein, Phys. Lett. **B486**, 86 (2000), [hep-ph/0005124].

[151] A. K. Leibovich, I. Low and I. Z. Rothstein, Phys. Lett. **B513**, 83 (2001), [hep-ph/0105066].

[152] A. H. Hoang, Z. Ligeti and M. Luke, Phys. Rev. **D71**, 093007 (2005), [hep-ph/0502134].

[153] B. O. Lange, M. Neubert and G. Paz, JHEP **10**, 084 (2005), [hep-ph/0508178].

[154] B. O. Lange, JHEP **01**, 104 (2006), [hep-ph/0511098].

[155] M. Neubert, Phys. Lett. **B612**, 13 (2005), [hep-ph/0412241].

[156] Z. Ligeti, I. W. Stewart and F. J. Tackmann, Phys. Rev. **D78**, 114014 (2008), [arXiv:0807.1926].

[157] P. Gambino, K. J. Healey and C. Mondino, Phys. Rev. **D94**, 1, 014031 (2016), [arXiv:1604.07598].

[158] B. O. Lange, M. Neubert and G. Paz, Phys. Rev. **D72**, 073006 (2005), [hep-ph/0504071].

[159] P. Gambino *et al.*, JHEP **10**, 058 (2007), [arXiv:0707.2493].

[160] J. R. Andersen and E. Gardi, JHEP **01**, 097 (2006), [hep-ph/0509360].

[161] M. Beneke *et al.*, JHEP **06**, 071 (2005), [hep-ph/0411395].

[162] C. Greub, M. Neubert and B. D. Pecjak, Eur. Phys. J. **C65**, 501 (2010), [arXiv:0909.1609].

[163] M. Brucherseifer, F. Caola and K. Melnikov, Phys. Lett. **B721**, 107 (2013), [arXiv:1302.0444].

[164] T. Mannel and S. Recksiegel, Phys. Rev. **D60**, 114040 (1999), [hep-ph/9904475].

[165] U. Aglietti *et al.*, Eur. Phys. J. **C59**, 831 (2009), [arXiv:0711.0860].

[166] C. W. Bauer, Z. Ligeti and M. E. Luke, Phys. Rev. **D64**, 113004 (2001), [hep-ph/0107074].

[167] C. W. Bauer, Z. Ligeti and M. E. Luke, Phys. Lett. **B479**, 395 (2000), [hep-ph/0002161].

[168] I. I. Y. Bigi and N. G. Uraltsev, Nucl. Phys. **B423**, 33 (1994), [hep-ph/9310285].

[169] M. B. Voloshin, Phys. Lett. **B515**, 74 (2001), [hep-ph/0106040].

[170] Z. Ligeti, M. Luke and A. V. Manohar, Phys. Rev. **D82**, 033003 (2010), [arXiv:1003.1351].

[171] P. Gambino and J. F. Kamenik, Nucl. Phys. **B840**, 424 (2010), [arXiv:1004.0114].

[172] J. L. Rosner *et al.* (CLEO), Phys. Rev. Lett. **96**, 121801 (2006), [hep-ex/0601027].

[173] L. Cao *et al.* (Belle), Phys. Rev. D **104**, 1, 012008 (2021), [arXiv:2102.00020].

[174] B. Aubert *et al.* (BaBar), in "23rd International Symposium on Lepton-Photon Interactions at High Energy (LP07)," (2007), [arXiv:0708.1753].

[175] J. P. Lees *et al.* (BaBar), Phys. Rev. D **86**, 032004 (2012), [arXiv:1112.0702].

[176] M. Hohmann *et al.* (Belle) (2023), [arXiv:2311.00458].

[177] R. Barate *et al.* (ALEPH), Eur. Phys. J. **C6**, 555 (1999).

[178] M. Acciarri *et al.* (L3), Phys. Lett. **B436**, 174 (1998).

[179] G. Abbiendi *et al.* (OPAL), Eur. Phys. J. **C21**, 399 (2001), [hep-ex/0107016].

[180] P. Abreu *et al.* (DELPHI), Phys. Lett. **B478**, 14 (2000), [hep-ex/0105054].

[181] A. Bornheim *et al.* (CLEO), Phys. Rev. Lett. **88**, 231803 (2002), [hep-ex/0202019].

[182] A. Limosani *et al.* (Belle), Phys. Lett. **B621**, 28 (2005), [hep-ex/0504046].

[183] J. P. Lees *et al.* (BaBar), Phys. Rev. **D95**, 7, 072001 (2017), [arXiv:1611.05624].

[184] B. Aubert *et al.* (BaBar), Phys. Rev. Lett. **95**, 111801 (2005), [Erratum: Phys. Rev. Lett.97,019903(2006)], [hep-ex/0506036].

[185] R. V. Kowalewski and S. Menke, Phys. Lett. **B541**, 29 (2002), [hep-ex/0205038].

[186] J. P. Lees *et al.* (BaBar), Phys. Rev. **D86**, 032004 (2012), [arXiv:1112.0702].

[187] I. Bizjak *et al.* (Belle), Phys. Rev. Lett. **95**, 241801 (2005), [hep-ex/0505088].

[188] P. Urquijo *et al.* (Belle), Phys. Rev. Lett. **104**, 021801 (2010), [arXiv:0907.0379].

[189] B. Aubert *et al.* (BaBar), Phys. Rev. Lett. **96**, 221801 (2006), [hep-ex/0601046].

[190] L. Cao *et al.* (Belle), Phys. Rev. Lett. **127**, 26, 261801 (2021), [arXiv:2107.13855].

[191] L. Cao *et al.* (Belle) (2023), [arXiv:2303.17309].

[192] A. Sibidanov *et al.* (Belle), Phys. Rev. **D88**, 3, 032005 (2013), [arXiv:1306.2781].

[193] B. Aubert *et al.* (BaBar), Phys. Rev. Lett. **90**, 181801 (2003), [eConfC0304052,WG117(2003)], [hep-ex/0301001].

[194] T. Hokuue *et al.* (Belle), Phys. Lett. **B648**, 139 (2007), [hep-ex/0604024].

[195] B. Aubert *et al.* (BaBar), Phys. Rev. **D79**, 052011 (2009), [arXiv:0808.3524].

[196] J. P. Lees *et al.* (BaBar), Phys. Rev. **D88**, 7, 072006 (2013), [arXiv:1308.2589].

[197] J. P. Lees *et al.* (BaBar), Phys. Rev. **D87**, 3, 032004 (2013), [Erratum: Phys. Rev.D87,no.9,099904(2013)], [arXiv:1205.6245].

[198] C. Schwanda *et al.* (Belle), Phys. Rev. Lett. **93**, 131803 (2004), [hep-ex/0402023].

[199] N. E. Adam *et al.* (CLEO), Phys. Rev. Lett. **99**, 041802 (2007), [hep-ex/0703041].

[200] S. B. Athar *et al.* (CLEO), Phys. Rev. **D68**, 072003 (2003), superceded by Ref. [201], [hep-ex/0304019].

[201] R. Gray *et al.* (CLEO), Phys. Rev. **D76**, 012007 (2007), [Addendum: Phys. Rev.D76,no.3,039901(2007)], [hep-ex/0703042].

[202] P. del Amo Sanchez *et al.* (BaBar), Phys. Rev. **D83**, 032007 (2011), supercedes Ref. [203], [arXiv:1005.3288].

[203] B. Aubert *et al.* (BaBar), Phys. Rev. **D72**, 051102 (2005), [hep-ex/0507003].

[204] P. del Amo Sanchez *et al.* (BaBar), Phys. Rev. **D83**, 052011 (2011), updated in Ref. [205], [arXiv:1010.0987].

[205] J. P. Lees *et al.* (BaBar), Phys. Rev. **D86**, 092004 (2012), [arXiv:1208.1253].

[206] J. A. Bailey *et al.* (Fermilab Lattice, MILC), Phys. Rev. **D92**, 1, 014024 (2015), [arXiv:1503.07839].

[207] A. Bazavov *et al.* (Fermilab Lattice, MILC), Phys. Rev. **D100**, 3, 034501 (2019), [arXiv:1901.02561].

[208] C. M. Bouchard *et al.*, Phys. Rev. **D90**, 054506 (2014), [arXiv:1406.2279].

[209] J. M. Flynn *et al.*, Phys. Rev. **D91**, 7, 074510 (2015), [arXiv:1501.05373].

[210] J. M. Flynn *et al.* (RBC/UKQCD), Phys. Rev. D **107**, 11, 114512 (2023), [arXiv:2303.11280].

[211] B. Colquhoun *et al.* (JLQCD), Phys. Rev. D **106**, 5, 054502 (2022), [arXiv:2203.04938].

[212] A. X. El-Khadra, A. S. Kronfeld and P. B. Mackenzie, Phys. Rev. D **55**, 3933 (1997), [hep-lat/9604004].

[213] A. Berns and H. Lamm, JHEP **12**, 114 (2018), [arXiv:1808.07360].

[214] N. Gubernari, D. van Dyk and J. Virto, JHEP **02**, 088 (2021), [arXiv:2011.09813].

[215] T. Blake *et al.*, Phys. Rev. D **108**, 9, 094509 (2023), [arXiv:2205.06041].

[216] N. Gubernari *et al.*, JHEP **09**, 133 (2022), [arXiv:2206.03797].

[217] T. Becher and R. J. Hill, Phys. Lett. **B633**, 61 (2006), [hep-ph/0509090].

[218] M. C. Arnesen *et al.*, Phys. Rev. Lett. **95**, 071802 (2005), [hep-ph/0504209].

[219] M. A. Shifman, A. I. Vainshtein and V. I. Zakharov, Nucl. Phys. **B147**, 385 (1979); M. A. Shifman, A. I. Vainshtein and V. I. Zakharov, Nucl. Phys. **B147**, 448 (1979).

[220] P. Ball and R. Zwicky, Phys. Rev. **D71**, 014015 (2005), [hep-ph/0406232].

[221] G. Duplancic *et al.*, JHEP **04**, 014 (2008), [arXiv:0801.1796].

[222] A. Bharucha, JHEP **05**, 092 (2012), [arXiv:1203.1359].

[223] A. V. Rusov, Eur. Phys. J. **C77**, 7, 442 (2017), [arXiv:1705.01929].

[224] I. Sentitemsu Imsong *et al.*, JHEP **02**, 126 (2015), [arXiv:1409.7816].

[225] D. Leljak, B. Melić and D. van Dyk, JHEP **07**, 036 (2021), [arXiv:2102.07233].

[226] H. Ha *et al.* (Belle), Phys. Rev. **D83**, 071101 (2011), [arXiv:1012.0090].

[227] B. Aubert *et al.* (BaBar), Phys. Rev. Lett. **101**, 081801 (2008), [arXiv:0805.2408].

[228] W. S. Brower and H. P. Paar, Nucl. Instrum. Meth. **A421**, 411 (1999), [hep-ex/9710029].

[229] P. Ball, eConf **C070512**, 016 (2007), [arXiv:0705.2290].

[230] J. M. Flynn and J. Nieves, Phys. Lett. **B649**, 269 (2007), [hep-ph/0703284].

[231] S. Aoki *et al.*, Eur. Phys. J. **C77**, 2, 112 (2017), [arXiv:1607.00299].

[232] A. Biswas *et al.*, JHEP **07**, 082 (2021), [arXiv:2103.01809].

[233] R. Aaij *et al.* (LHCb), Phys. Rev. Lett. **126**, 8, 081804 (2021), [arXiv:2012.05143].

[234] A. Khodjamirian and A. V. Rusov, JHEP **08**, 112 (2017), [arXiv:1703.04765].

[235] A. Bazavov *et al.* (Fermilab Lattice, MILC), Phys. Rev. D **107**, 9, 094516 (2023), [arXiv:2212.12648].

[236] C. Bolognani, D. van Dyk and K. K. Vos (2023), [arXiv:2308.04347].

[237] T. Feldmann and M. W. Y. Yip, Phys. Rev. **D85**, 014035 (2012), [Erratum: Phys. Rev.D86,079901(2012)], [arXiv:1111.1844].

[238] W. Detmold, C. Lehner and S. Meinel, Phys. Rev. **D92**, 3, 034503 (2015), [arXiv:1503.01421].

[239] R. Aaij *et al.* (LHCb), Nature Phys. **11**, 743 (2015), [arXiv:1504.01568].

[240] M. Ablikim *et al.* (BESIII), Phys. Rev. Lett. **116**, 5, 052001 (2016), [arXiv:1511.08380].

[241] R. Aaij *et al.* (LHCb), Phys. Rev. **D96**, 11, 112005 (2017), [arXiv:1709.01920].

[242] M. Tanaka, Z. Phys. **C67**, 321 (1995), [hep-ph/9411405].

[243] H. Itoh, S. Komine and Y. Okada, Prog. Theor. Phys. **114**, 179 (2005), [hep-ph/0409228].

[244] U. Nierste, S. Trine and S. Westhoff, Phys. Rev. **D78**, 015006 (2008), [arXiv:0801.4938].

[245] M. Tanaka and R. Watanabe, Phys. Rev. **D82**, 034027 (2010), [arXiv:1005.4306].

[246] A. Datta, M. Duraisamy and D. Ghosh, Phys. Rev. **D86**, 034027 (2012), [arXiv:1206.3760].

[247] D. Becirevic, N. Kosnik and A. Tayduganov, Phys. Lett. **B716**, 208 (2012), [arXiv:1206.4977].

[248] S. Fajfer *et al.*, Phys. Rev. Lett. **109**, 161801 (2012), [arXiv:1206.1872].

[249] A. Crivellin, C. Greub and A. Kokulu, Phys. Rev. **D86**, 054014 (2012), [arXiv:1206.2634].

[250] M. Bauer and M. Neubert, Phys. Rev. Lett. **116**, 14, 141802 (2016), [arXiv:1511.01900].

[251] I. Doršner *et al.*, Phys. Rept. **641**, 1 (2016), [arXiv:1603.04993].

[252] A. Celis *et al.*, Phys. Lett. **B771**, 168 (2017), [arXiv:1612.07757].

[253] S. Jaiswal, S. Nandi and S. K. Patra, JHEP **12**, 060 (2017), [arXiv:1707.09977].

[254] J. P. Lees *et al.* (BaBar), Phys. Rev. Lett. **109**, 101802 (2012), [arXiv:1205.5442].

[255] J. P. Lees *et al.* (BaBar), Phys. Rev. **D88**, 7, 072012 (2013), [arXiv:1303.0571].

[256] M. Huschle *et al.* (Belle), Phys. Rev. **D92**, 7, 072014 (2015), [arXiv:1507.03233].

[257] S. Hirose *et al.* (Belle), Phys. Rev. Lett. **118**, 21, 211801 (2017), [arXiv:1612.00529].

[258] G. Caria *et al.* (Belle), Phys. Rev. Lett. **124**, 16, 161803 (2020), [arXiv:1910.05864].

[259] I. Adachi *et al.* (Belle-II) (2024), [arXiv:2401.02840].

[260] R. Aaij *et al.* (LHCb), Phys. Rev. D **108**, 1, 012018 (2023), [arXiv:2305.01463].

[261] R. Aaij *et al.* (LHCb), Phys. Rev. Lett. **131**, 111802 (2023), [arXiv:2302.02886].

[262] M. Blanke, PoS **LeptonPhoton2019**, 015 (2019), [arXiv:1908.09713].

[263] S. Descotes-Genon, PoS **ALPS2019**, 016 (2020).

[264] D. London and J. Matias, Ann. Rev. Nucl. Part. Sci. **72**, 37 (2022), [arXiv:2110.13270].

[265] J. G. Korner and G. A. Schuler, Z. Phys. **C46**, 93 (1990).

[266] A. Abdesselam *et al.* (Belle), in "10th International Workshop on the CKM Unitarity Triangle (CKM 2018) Heidelberg, Germany, September 17-21, 2018," (2019), [arXiv:1903.03102].

[267] A. Matyja *et al.* (Belle), Phys. Rev. Lett. **99**, 191807 (2007), [arXiv:0706.4429].

[268] A. Bozek *et al.* (Belle), Phys. Rev. **D82**, 072005 (2010), [arXiv:1005.2302].

[269] M. Tanaka and R. Watanabe, Phys. Rev. **D87**, 3, 034028 (2013), [arXiv:1212.1878].

[270] R. Aaij *et al.* (LHCb), Phys. Rev. Lett. **120**, 12, 121801 (2018), [arXiv:1711.05623].

[271] J. Harrison, C. T. H. Davies and A. Lytle (LATTICE-HPQCD), Phys. Rev. Lett. **125**, 22, 222003 (2020), [arXiv:2007.06956].

[272] J. Harrison, C. T. H. Davies and A. Lytle (HPQCD), Phys. Rev. D **102**, 9, 094518 (2020), [arXiv:2007.06957].

[273] S. Hirose *et al.* (Belle), Phys. Rev. **D97**, 1, 012004 (2018), [arXiv:1709.00129].

[274] I. Adachi *et al.* (Belle-II) (2023), [arXiv:2311.07248].

[275] M. Freytsis, Z. Ligeti and J. T. Ruderman, Phys. Rev. D **92**, 5, 054018 (2015), [arXiv:1506.08896].

[276] M. Rahimi and K. K. Vos, JHEP **11**, 007 (2022), [arXiv:2207.03432].

[277] Z. Ligeti, M. Luke and F. J. Tackmann, Phys. Rev. D **105**, 7, 073009 (2022), [arXiv:2112.07685].

[278] I. Adachi *et al.* (Belle-II), Phys. Rev. Lett. **131**, 18, 181801 (2023), [arXiv:2308.02023].

[279] L. Aggarwal *et al.* (Belle-II), Phys. Rev. Lett. **131**, 5, 051804 (2023), [arXiv:2301.08266].

[280] P. Gambino and S. Hashimoto, Phys. Rev. Lett. **125**, 3, 032001 (2020), [arXiv:2005.13730].

[281] P. Gambino *et al.*, JHEP **07**, 083 (2022), [arXiv:2203.11762].

[282] A. Barone *et al.*, JHEP **07**, 145 (2023), [arXiv:2305.14092].

[283] Y. Amhis *et al.* (HFLAV), Eur. Phys. J. **C77**, 12, 895 (2017), [arXiv:1612.07233].